JUL 27 1970

AEDC-TR-70-131

cy. 2

A CLASSICAL MODEL FOR GAS-SURFACE INTERACTION

M. R. Busby, J. D. Haygood, and C. H. Link, Jr.

ARO, Inc.

July 1970

This document has been approved for public release and sale; its distribution is unlimited.

VON KÁRMÁN GAS DYNAMICS FACILITY
ARNOLD ENGINEERING DEVELOPMENT CENTER
AIR FORCE SYSTEMS COMMAND
ARNOLD AIR FORCE STATION, TENNESSEE

PROPERTY OF U S AIR FORCE
AEDC LIBRARY
F40600-71-C-0002

NOTICES

When U. S. Government drawings specifications, or other data nre used for any purpose other than a definitely related Government procurement operation, the Government thereby incurs no responsibility nor any obligation whatsoever. and the fuct that the Govei nment may have formulated, furnished, or in any way supplied the said drawings, specifications, or other data, is not to be regarded by implication or otherwise, or in any manner licensing the holder or any other person or corporation, or conveying any rights or permission to manufacture, use. or sell any patented invention that may in any way be related thereto.

Qualified users may obtain copies of this report from the Defense Documentation Center.

References to named commercial products in this report are not to be considered in any sense as an endorsement of the product by the United States Air Force or the Government.

A CLASSICAL MODEL FOR GAS-SURFACE INTERACTION

M. R. Busby, J. D. Haygood, and C. H. Link, Jr.
ARO, Inc.

This document has been approved for public release and sale; its distribution is unlimited.

FOREWORD

The research presented in this report was sponsored by the Arnold Engineering Development Center (AEDC), Air Force Systems Command (AFSC), Arnold Air Force Station, Tennessee, under Program Element 64719F.

The results reported herein were obtained by ARO, Inc. (a subsidiary of Sverdrup & Parcel and Associates, Inc.), contract operator of the AEDC, AFSC, under Contract F40600-71-C-0002. The research was conducted from July 1969 to March 1970 under ARO Project No. SW3003, and the manuscript was submitted for publication on April 3, 1970.

The authors wish to express gratitude to Caroline Neal for her aid in the computer analysis.

This technical report has been reviewed and approved.

Michael G. Buja
First Lieutenant, USAF
Research Division
Directorate of Plans
and Technology

Harry L. Maynard
Colonel, USAF
Research Division
Director of Plans
and Technology

ABSTRACT

A classical theoretical model for gas-surface interaction has been formulated and tested using the experimental data for the gaseous-argon, solid-argon system. The theoretical interaction is modeled as the collision of hard spheres with the inclusion of surface temperature and an attractive surface field energy which is the only adjustable parameter in the formulation. The theoretical results from this exceedingly simple model exhibit nearly every characteristic of the available experimental data for argon. Several general conclusions about the actual argon-argon interaction were made. First, classical mechanics appeared to provide a useful description for the interaction. Second, a hard sphere model was adequate to predict the gas-solid collision properties over the range of experimental conditions although the theoretical spatial distributions are narrower than those experimentally measured. Third, in order to match the experimental capture coefficient data, the magnitude of the surface field energy was nearer the heat of sublimation rather than the Lennard-Jones or Morse potential well-depth values.

CONTENTS

		Page
	ABSTRACT	iii
	NOMENCLATURE	vii
I.	INTRODUCTION	1
	1.1 Basic Considerations	1
	1.2 Classical Scattering Theories Applicable to the Present Work	2
II.	FORMULATION OF A MATHEMATICAL HARD SPHERE MODEL	3
	2.1 Assumptions of the Model	3
	2.2 Details of the Model and Computation	4
	2.2.1 The Macrosurface Interaction	4
	2.2.2 The Microsurface Interaction	5
	2.2.3 The Normal Polar Directional Map	5
	2.3 Spatial Distributions	5
	2.3.1 General Features of the Scattering Patterns	5
	2.3.2 Hard Sphere Results	6
III.	FORMULATION OF A PHYSICAL HARD SPHERE MODEL	6
	3.1 The Surface Field Energy	6
	3.1.1 Inclusion of the Surface Field Energy in the Model	6
	3.1.2 Theoretical Estimation of the Surface Field Energy	7
	3.1.3 Spatial Distributions and Capture Coefficients	8
	3.2 The Surface Temperature	9
	3.2.1 Exchange of Micronormal Momentum	9
	3.2.2 Spatial Distributions and Capture Coefficients	10
	3.3 Summary of the Physical Hard Sphere Model	10
IV.	COMPARISON WITH EXPERIMENTAL DATA	10
	4.1 The Beam Capture Coefficient	10
	4.1.1 Variation of Beam Incidence Angle	11
	4.1.2 Variation of Beam Incident Energy	11
	4.1.3 Variation of Surface Temperature	11
	4.2 The Spatial Distributions	12
V.	CONCLUSIONS	13
	REFERENCES	15

APPENDIXES

I. ILLUSTRATIONS

Figure

1.	Surface Configurations	19
2.	Relation of Surface Modules to Surface Arrays	19
3.	Surface Modules	20
4.	Randomization of the Surface Module	21
5.	Normal Polar Directional Map	22
6.	Orientation Parameters for the Reflected Beam	23

Figure Page

7. Variation of the In-Plane Normalized Spatial Distributions with Number of Trajectories 24
8. Comparison of the In-Plane Normalized Spatial Distributions of the Hexagonal and Square Surface Arrays 25
9. Square-Well Potential 26
10. Trajectory Alterations due to the Square-Well Potential 27
11. Geometry for the Estimation of the Surface Field Energy 28
12. Heat of Sublimation for Solid Argon at Equilibrium 29
13. In-Plane Normalized Spatial Distributions for Various Surface Field Energies 30
14. Beam Capture Coefficient for Various Surface Field Energies 31
15. Probability for a Surface Velocity 32
16. In-Plane Normalized Spatial Distributions for Various Surface Temperatures 33
17. In-Plane Normalized Spatial Distributions for Various Angles of Incidence 34
18. Comparison of the Normalized In-Plane and Out-of-Plane Spatial Distributions 35
19. Beam Capture Coefficient for Various Angles of Incidence–Comparison of Theory and Experiment 36
20. Beam Capture Coefficient for Various Beam Energies–Comparison of Theory and Experiment 37
21. Beam Capture Coefficient for Various Surface Temperatures–Comparison of Theory and Experiment 38
22. Comparison of the Normalized Heat of Sublimation and Empirical Attractive Surface Field Energy for Various Surface Temperatures 39
23. Normalized In-Plane Spatial Distribution for θ_i = 70 deg and E_i = 0.50 ev 40
24. Normalized In-Plane bution for θ_i = 60 deg and E_i = 0.50 ev 41
25. Normalized In-Plane Spatial Distribution for θ_i = 30 deg and E_i = 0.50 ev 42
26. Normalized In-Plane Spatial Distribution for θ_i = 60 deg and E_i = 0.43 ev 43
27. Normalized In-Plane Spatial Distribution for θ_i = 60 deg and E_i = 0.37 ev 44

II. TABLE

I. Estimated Values of the Surface Field Energy Based on a Lennard-Jones Potential 45

NOMENCLATURE

C_b	Experimental beam capture coefficient
d	Interatomic spacing
E_A	Attractive surface field energy
E_I	Total incident beam energy, $E_i + E_A$
E_i	Incident beam energy
E_F	Total final exiting atom energy, $E_f - E_A$
E_f	Final exiting atom energy
F	Fraction of surface atoms with kinetic energy equal to or greater than E_A
H_s	Equilibrium heat of sublimation
$\vec{I}$	Incident ray vector
I_N	Micronormal component of momentum
I_T	Microtangential component of momentum
k	Boltzmann constant
m	Mass of gas and surface atoms
n	Number of atoms per unit cell
$\dot{n}_i$	Total experimental incident flux
$\dot{n}_r$	Total experimental reflected flux
P	Randomization angle for surface modules
P_s	Probability that a surface atom has a velocity less than V_n
R	Radius of surface module spherical cap
r_o	Lennard-Jones well-depth distance
r	Center-to-center distance between two atoms
s	Height of gas atom above the surface

T_s	Surface temperature
V_n	Micronormal velocity
x, y, z	Macrocoordinate system
α, β, γ	Microcoordinate system
ϵ	Lennard-Jones or Morse well-depth parameter
ϕ	Out-of-plane or transverse plane angle
ρ	Number density per unit cell
τ	Depth of potential element below the surface
σ	Value of r when potential is zero
θ_i	Beam incidence angle (measured from macrosurface normal)
θ_I	Modified beam incidence angle
θ_f	Ray exit angle (measured from macrosurface normal)
θ_F	Modified ray exit angle
θ_r	Reflected in-plane angle
θ_{rm}	Angle of maximum reflected intensity

SECTION I
INTRODUCTION

1.1 BASIC CONSIDERATIONS

The purpose of this report is to show that a relatively simple classical model of gas-surface interaction is sufficient to describe many of the experimentally observed results. The essential feature of this model is the description of the surface. Since the concern is for the interaction at low pressures of individual molecules with the surface, the model of the surface should be on a molecular scale. It is probable that any solid surface, on a molecular scale, is highly complex. There are ledges, several molecules high, as well as dislocations and lattice vacancies. The lattice parameters are not the same in the surface as in the bulk material because of the asymmetry of the potential field at the surface. In fact, the formulation of a complete description of a solid surface would be extremely difficult if not impossible on a molecular scale.

In order to resolve this difficulty, consider the fraction of the surface which is simple in structure compared with the fraction which is complex. Since complex structures will generally have a higher energy than simple structures, there will be a driving force tending to eliminate the complex structures by conversion to simpler configurations. The result is that the majority of the surface area will consist of simple configurations when considering an area of only a few molecules. Since the range of intermolecular forces is short, it should be possible to construct a model of a surface, consisting of simple arrangements of the molecules, which will be adequate for a semiquantitative description of the gas-surface interaction. A further simplification may be realized by treating the case of a monatomic gas interacting with the solid phase of the same material. This would be the case for argon gas interacting with a solid-argon surface. Although the solid surface may be amorphous, it can be considered to be locally crystalline. The structure of crystalline argon has been found to be face centered cubic. Therefore, there are two possible surface arrangements, both planar. These are the square array and the hexagonal array. In this work, the collision of hard sphere argon atoms with a surface made up of hard sphere argon atoms in either or both surface arrangements is considered. Thus far the model is similar to that used by Goodman (Ref. 1); however, he assumed that the orientation of the surface array was constant, whereas in the current work, the surface orientation is chosen randomly for each incident atom. Further, the surface atoms are considered to have a Maxwellian energy distribution which allows an estimation of the effect of surface temperature. To complete the model, a square-well potential is used so that a probability of condensation of an incident atom may be calculated. This potential also has an effect on the spatial distribution of those atoms which are reflected.

This model has been incorporated into a Monte Carlo computer program, the results of which show a semiquantitative agreement with the experimental data. Several effects have not been included since these are thought to be of second order and would unduly complicate the computer program Among these are (1) motion of surface atoms into the surface, (2) the shape of the potential well, (3) departures of the surface from flatness, and (4) the width of the molecular beam. Of these effects, the most important

are believed to be the negative velocities of some surface atoms in a real surface and the departure of the real surface from flatness. By ignoring the possibility of negative surface atom velocities, the range of validity of the model is restricted to low surface temperatures, i.e., less than 50°K. The departure of a real surface from flatness is believed to be one of the reasons that the computer model gives narrower lobes than those observed experimentally.

1.2 CLASSICAL SCATTERING THEORIES APPLICABLE TO THE PRESENT WORK

Early studies of gas-surface interactions on a molecular scale quite naturally followed the development of the kinetic theory of gases. By 1910 the kinetic theory had suggested a family of parameters similar to the surface emissivity or absorptivity in radiation theory to describe the average effect of surfaces on gas flow without any model of the interaction or of the solid surface.

In 1914 Baule (Ref. 2) first attempted a model of the solid surface. He represented it as an array of noninteracting hard spheres initially at rest which were struck by hard sphere gas molecules. The interaction was instantaneous so that only one solid atom was involved per collision.

Following Baule, several gas-surface interaction theories were proposed based on both classical and the newly developed quantum mechanics. However, these models were generally one-dimensional, very complex, and dealt with energy transfer between the gas and the surface rather than the prediction of scattered spatial flux distributions. Only in recent years have more realistic three-dimensional scattering models been proposed.

At present, the most complete classical model of gas-surface interactions is that of Oman et al (Refs. 3, 4, and 5). The solid is represented by a regular array of lattice atoms, and it is assumed that the intermolecular forces applied to an incident gas atom may be described by a Lennard-Jones 6-12 potential summed over all solid atoms. By utilizing classical mechanics, the three-dimensional trajectory of a gas atom is determined by numerical computation. Results are obtained for the dependence of the reflected flux distributions and momentum transfer on the energy and angle of the incident atom, the point of impact, the mass ratio, the depth of the potential well, and the crystallographic structure of the solid surface. Oman has used a wide variety of conditions in this model, e.g., solids consisting of harmonic oscillators both coupled and uncoupled, realistic surface temperatures, other types of potential functions, etc., to study the relative importance of these phenomena. Although this model is perhaps the most general, its essential difficulty is that it is so complex and requires long computation times which limit the number of trajectories available for study.

A similar study has been performed recently by Goodman (Ref. 1) who used an array of hard spheres in a manner similar to the present work. The problem is simplified by assuming a hard sphere intermolecular potential for the gas-solid interaction. Also, the solid atoms are assumed to behave as independent hard spheres that are initially at rest. The results illustrate the dependence of the scattering pattern, as well as the momentum and energy transfer, on the energy and angle of the incident atoms, the mass ratio, the diameters of the spheres, and the crystallographic structure of the solid surface.

A more flexible, simple model designed to predict the variation of scattered flux distributions with the ratio of the surface to gas temperature has been developed by Logan, Keck, and Stickney (Refs. 6 and 7). They represent the surface of the solid as a set of independent smooth, plane, hard cubes whose velocity distribution normal to the surface is a one-dimensional Maxwell-Boltzmann distribution appropriate to the surface temperature. When a gas molecule strikes the surface cube at a given incident angle, the momentum exchange normal to the surface follows the law of hard spheres. The tangential component of momentum is left unchanged by the interaction. The scattered lobe shape depends on the incidence angle, the mass ratio, and the ratio of gas to surface temperatures. Agreement between the predicted angles of maximum lobe intensity and the measured values for argon-platinum argon-silver, etc., is fairly good.

A classical three-dimensional model of the interaction of rare gas atoms with clean metal surfaces at satellite velocities has been presented by Jackson (Ref. 8). The surface is assumed to be an ideal crystal plane with no thermal motion. The surface atoms are decoupled in collision and resume their original position after a collision. The surface field is modeled by repulsive hard sphere collisions at an appropriate radius of interaction and by a smooth normal attractive field due to the entire semi-infinite solid. Aside from the parameters which are fixed in an experiment, the model has two adjustable parameters: the interaction radius and the attractive field energy. A series of numerical experiments was performed, and flux and velocity distributions were found for a wide variety of situations.

SECTION II
FORMULATION OF A MATHEMATICAL HARD SPHERE MODEL

2.1 ASSUMPTIONS OF THE MODEL

An attempt has been made to analytically model the interaction of an inert, monatomic gas with its own solid phase as basically the collisions of hard spheres. Since there are no closed form solutions for multiple body interactions, it was decided to utilize a Monte Carlo approach for the computation of trajectories using the assumptions listed below. For trajectories from a surface at zero degree Kelvin, three random numbers are required: two to select the point of collision and one to specify the surface orientation. For surfaces not at zero degree, an additional random number is required for each encounter with a surface atom to select the energy exchange. The following assumptions have been made for a simplified hard sphere model:

Assumption 1. The validity of the classical mechanics approximation is assumed. Although this is an open question and cannot be proved or disproved at present, classical models have had some significant successes in experimental comparisons with other gas-surface systems.

Assumption 2. In spite of the enormous difficulty of mathematically describing a surface, a useful definition of a collision between a gas molecule and a surface can be proposed if one considers that the gas molecule interacts only with a very small area of the surface. Thus, short range crystal order is assumed even if the actual surface is

amorphous. With this assumption, there remain only two possibilities for the surface configuration, i.e., hexagonal or square arrays (Fig. 1, Appendix I).

Assumption 3. Multiple collisions between an incident ray (molecule) and several surface atoms are possible. It is assumed that the gas molecule striking a square array remains in a square array until it leaves the surface and likewise for the hexagonal array. Since only a small fraction of the incident molecules will undergo more than two collisions in the surface, the assumption should not lead to serious error.

Assumption 4. The surfaces of short range order are both molecularly flat (i.e., the centers of all the surface atoms on the average lie in a plane) and are parallel to the macrosurface. This assumption will have the effect of making the calculated spatial distributions of reflected molecules narrower than the observed distributions.

Assumption 5. The surface atoms interact with the gas atoms as decoupled particles, i.e., forces among the surface atoms are negligible in the collisions.

Assumption 6. All collisions of the incident gas atom are with surface atoms in their equilibrium positions.

Assumption 7. The surface atoms have no initial velocities before collision. A more general case is formulated in Section 3.2 for surface atoms having a Maxwell-Boltzmann velocity distribution corresponding to the surface temperature.

Assumption 8. The repulsive part of the interaction is represented by a hard sphere collision. In Section 3.1, an attractive surface field energy is included in the model.

2.2 DETAILS OF THE MODEL AND COMPUTATION

2.2.1 The Macrosurface Interaction

If the radius of the incoming gas atom is reduced to zero and the radius of the surface atom is doubled, there will be no change in the resultant trajectories, but the geometry is simplified by this transformation. The relation of a transformed surface module to its corresponding surface array (square or hexagonal) is shown in Fig. 2. In Fig. 3 the surface modules, the coordinate systems, and the micro- and macrosurfaces used in the analytical formulation of the model are depicted.

The point of incidence of an incoming ray (molecule) on the macrosurface of the module is randomly selected. The orientation of the surface module relative to the plane formed by the incident ray and the macrosurface normal is randomized by an angle P (Fig. 4). The angle P varies over a range from -45 to 45 deg for the square array, and from -30 to 30 deg for the hexagonal array; the ranges were selected on the basis of symmetry.

For a given angle of incidence and randomizing angle P, the direction cosines of the incident ray are determined. The magnitude (i.e. velocity) of the incident ray vector, $\vec{I}$, is given by $\sqrt{2E_i/m}$ where E_i is the incident energy and m is the mass of the incoming gas atom. Thus, the coordinates of the point of incidence and the direction cosines of the incident ray are determined with respect to the macrosurface.

2.2.2 The Microsurface Interaction

To follow the ray from the macrosurface to the point of collision on the microsurface, the macrocoordinate system is subjected to a geometric transformation to a microcoordinate system which is normal and tangent to the surface of the spherical cap, i.e., microsurface (Fig. 3). The tangential component, I_T, of the momentum is conserved at the microsurface. The normal component, I_N, of the momentum is exchanged with the microsurface. Since the surface is assumed to be initially at rest (Assumption 7), the micronormal component of momentum of the reflected atom is zero after the collision.

After the exchange of the micronormal momentum and conservation of the microtangential momentum, the microcoordinate system is transformed once again to the macrocoordinate system, and a new set of direction cosines is computed. If the direction of the exiting ray is such that it intersects the macrosurface, the final energy and trajectory are computed, and the ray is placed in the normal polar directional map. However, if the direction is such that the gas atom exits through the side of the surface module, the computer shifts the module and treats the exiting gas atom as a new incident ray.

2.2.3 The Normal Polar Directional Map

Those exiting atoms which intersect the macrosurface are placed in a spatial distribution map. The normal polar directional map is shown in Fig. 5. The map is divided into cells of constant area simulating the experimental condition of a constant area flux detector. The cells are defined by dividing the cosine of the polar angle (range 0 to 1 deg) into 25 equal increments and by dividing the azimuthal angle (range 0 to 180 deg) into 18 equal increments, giving a total of 450 cells each covering $\pi/450$ steradians.

2.3 SPATIAL DISTRIBUTIONS

2.3.1 General Features of the Scattering Patterns

The theoretical results presented in this and succeeding sections are representative samples chosen to show the effects of the number of trajectories and the surface arrays on the spatial distributions. For these sample sets, only a representative subset of data is presented; in particular, results in two characteristic planes which correspond to those for which the experimental data are available. With reference to the coordinate system in Fig. 6, these planes are:

1. The principal plane ($\phi = 0$)

2. The transverse lobal plane ($\theta_r = \theta_{rm}$)

The angle θ_{rm} refers to the position in the principal plane where the reflected intensity is a maximum. In-plane scattering is displayed in the principal plane, and out-of-plane scattering is presented by way of the transverse lobal plane (Fig. 6). Input conditions for the computer program are the incident angle, incident energy, and surface array. With the formulation of the physical hard sphere model (Section III), the inputs of surface attractive field energy and surface temperature are added.

2.3.2 Hard Sphere Results

Since spurious results could possibly arise because of statistical effects, one must have sufficient trajectories to produce adequate and accurate scattering distributions. Since the convergence of the Monte Carlo technique used in the mathematical formulation of the model is unknown a priori, one must find the distribution for increasing numbers of trajectories and note how the distribution changes. A range of trajectory numbers was calculated (10,000, 20,000, 40,000) for an incident angle, θ_i, of 70 deg and an incident energy, E_i, of 0.5 ev. The in-plane scattering distributions for these cases are presented in Fig. 7. By assuming the 40,000 trajectory case to be the most accurate, it is observed that the 10,000 and 20,000 cases are a very good approximation to the 40,000 case. However, there is no guarantee that the same number of trajectories will yield uniformly valid distributions, and thus throughout the present work any unusual distribution was pursued to higher trajectory numbers to verify its validity or to eliminate it as spurious.

The cases presented in Fig. 7 are equally divided between the hexagonal and square surface arrays. A comparison of the in-plane distributions of these arrays is presented in Fig. 8. Scattering from the square array gives a slightly broader distribution and more pronounced "diffraction" lobes than the hexagonal array. Nevertheless, there are no important differences between the two scattering patterns, and results in the following sections will be divided evenly between the hexagonal and square arrays.

SECTION III
FORMULATION OF A PHYSICAL HARD SPHERE MODEL

3.1 THE SURFACE FIELD ENERGY

3.1.1 Inclusion of the Surface Field Energy in the Model

The interaction of an incident gas atom with a surface consists of two parts: a long range attractive part and a short range repulsive part. To include the effect of an attractive surface field energy, E_A, in the model, a square-well potential function is assumed (Fig. 9), and its alterations of the energies and trajectories of the gas atoms are the criteria proposed by Goodman (Ref. 9). Thus, to the initial incoming energy, E_i, a constant attractive potential energy, E_A, is added, i.e., conservation of energy at the macrosurface requires

$$E_I = E_i + E_A$$

Also the trajectory of the incoming molecule is changed at the macrosurface by considering an energy balance associated with the macronormal direction (Fig. 10),

$$E_I \cos^2 \theta_I = E_i \cos^2 \theta_i + E_A$$

The repulsive part of the interaction is still represented by a hard sphere collision as in the initial model. The microtangential component of momentum is conserved, whereas the micronormal component of the incoming gas atom is exchanged with the surface.

After having undergone the energy exchange in the repulsive interaction, the attractive potential decreases the energy, E_f, of the exiting gas atom, i.e., conservation of energy at the macrosurface requires

$$E_F = E_f - E_A$$

Also, an energy balance associated with the micronormal direction alters the trajectory by

$$E_F \cos^2 \theta_F = E_f \cos^2 \theta_f - E_A$$

If the final exiting energy, E_F, is less than the attractive potential energy, E_A, then the gas atom is assumed to be captured by the surface. If $E_F > E_A$ and the final exiting angle, θ_F, is less than 90 deg (θ_F is measured with respect to the surface macronormal), then the gas atom escapes. However, if $E_F > E_A$ and $\theta_F \geq 90$ deg, the gas atom "hops" on the surface.

3.1.2 Theoretical Estimation of the Surface Field Energy

The attractive potential energy, E_A, plays an important role in gas-surface interactions. Unfortunately, the determination of a definitive value of E_A with enough accuracy to justify its confident use in a gas-surface interaction theory is not currently possible. Nevertheless, attempts have been made to determine reasonable values of the surface field energy.

Perhaps the most obvious method of evaluating E_A is by integration of a free space potential over the semi-infinite solid (Ref. 10). That is, it is assumed that an interatomic potential acts between a gas atom and each element of the solid, and the total potential acting on the gas atom is obtained by integrating over all elements in the solid. By using the attractive part of the Lennard-Jones potential, i.e., $4\epsilon\sigma^6/r^6$ where ϵ is the well-depth, r is the center-to-center distance between two atoms, and σ is the value of r when the potential is zero, the surface field energy is estimated to be

$$E_A = -4\epsilon\sigma^6\rho \int_0^\infty \int_0^\infty \int_0^{2\pi} \frac{R\,dR\,d\theta\,d\tau}{[(s+\tau)^2 + R^2]^3} = \frac{2\epsilon\sigma^6\rho\pi}{3s^3}$$

The integration has been done in a cylindrical coordinate system (Fig. 11) where s is the height of the gas atom above the surface and τ is the depth of the potential element

below the surface. The parameter ρ is the number density per unit cell and is defined as $\rho = n/d^3$ where n is the number of atoms per unit cell and d is the interatomic spacing. In order to obtain a value of E_A, some value of s must be assumed to represent the distance from the surface where the field is cut off. There are a few likely possibilities for this cutoff: σ, d, and r_0 (Lennard-Jones well-depth distance = $2^{1/6}\sigma$). Unfortunately, there is no strong reason for using any one of these values and in effect a wide range of E_A values can be produced by various choices (Table I, Appendix II). Also, estimates of E_A depend on the Lennard-Jones potential parameters and are subject to any errors in the estimation of these parameters.

Some previous theories (Refs. 1 and 6) have generally assumed that E_A is the well-depth parameter, ϵ, associated with the Lennard-Jones 6-12 or Morse intermolecular potential functions for the gas-surface systems under study. However, such an assumption implies that the interaction involves only a single gas atom and a single surface atom, with the attractive effect of the neighboring surface atoms being neglected. Also, the validity of the application of the combination rule (Ref. 11) for obtaining the well-depth is questionable since in the previously studied systems the individual well-depths of the gas and surface atoms have very different values, e.g., for argon $\epsilon/k = 120°K$ and for tungsten, $\epsilon/k = 11{,}500°K$.

In the actual physical case, the surface field energy must be related to the macroscopic heat of sublimation, i.e., the amount of energy required, on the average, to take an atom from the bulk solid to the gaseous phase. Since the gas-solid interface is being considered, one would expect that the surface field energy is some fraction of the total heat of sublimation. The variation with surface temperature of the heat of sublimation of solid argon at equilibrium is shown in Fig. 12 (Ref. 12).

It is clear from this brief survey that E_A cannot be accurately determined. Thus, the attractive surface field energy will be an adjustable parameter in the model. Nevertheless, a comparison of the experimental and theoretical results based on various values of E_A is presented in the following sections.

3.1.3 Spatial Distributions and Capture Coefficients

The in-plane normalized spatial distributions for various values of the surface field energy are shown in Fig. 13. With the inclusion of E_A in the model, one observes that the scattering patterns become narrower than the distributions presented in Figs. 7 and 8. This narrowness is due to the high probability of capture of rays undergoing multiple collisions with the surface. For the case $E_A = 0$, multiple collision rays would have tended to broaden the spatial distribution since there was no capture mechanism. Also, the angle of maximum reflected intensity, θ_{rm}, becomes larger (i.e., lies closer to the surface) for the nonzero surface field energy cases. However, there was not an appreciable shift in θ_{rm} over the range of E_A values in Fig. 13.

The beam capture coefficient is a very strong function of the surface field energy as shown in Fig. 14. Its value varies for an argon model from 0.075 for $E_A/k = 257°K$ (value estimated from integration of the Lennard-Jones potential with $s = \sigma$; see Table I)

to 0.996 for $E_A/k = 934°K$ (value of the full heat of sublimation). In the following sections, a value of E_A will be selected which most closely reproduces the experimental results. However, it is encouraging that realistic values of the capture coefficient lie between the physical limits of the argon-argon system; i.e., $E_A/k = 120°K$ (Lennard-Jones well-depth) is the lower limit, whereas $E_A/k = 934°K$ (full heat of sublimation) is the upper limit.

3.2 THE SURFACE TEMPERATURE

3.2.1 Exchange of Micronormal Momentum

A more realistic surface can be modeled if the surface temperature is considered. It will be assumed that the surface atoms have an equilibrium distribution of velocities at the temperature of the solid. The exchange of the micronormal component of momentum between an incident gas and a surface atom is accomplished by calculating the probability, P_s, that a surface atom has a velocity less than a given velocity, say V_n, in the micronormal direction, i.e.,

$$P_s = \frac{1}{\sqrt{\pi}} \int_{-\infty}^{V_n} \exp\left\{-\frac{m}{2kT_s} V^2\right\} d\left(\frac{mV^2}{2kT_s}\right)^{1/2} = \frac{1}{2} + \frac{1}{2} \operatorname{erf}\left(\sqrt{\frac{m}{2kT_s}} V_n\right)$$

where T_s is the surface temperature and m is the mass of a surface atom. A sketch of P_s versus $\sqrt{m/2kT_s}\, V_n$ is shown in Fig. 15a. However, there is an attractive potential energy, E_A, associated with the collision of a gas atom on the surface array. Since a square-well potential is assumed, the corresponding impulsive attractive force tends to "pull" the surface atom toward the incoming gas atom. Those surface atoms having negative velocities in the micronormal direction will suffer a reversal of momentum due to the impulsive attractive force unless the energy associated with the micronormal direction is greater than E_A. Since the surface has an equilibrium distribution of energies, the fraction, F, of surface atoms with kinetic energy equal to or greater than E_A is given by Ref. 13,

$$F = 1 + \frac{2}{\sqrt{\pi}} \sqrt{\frac{E_A}{kT_s}}\, e^{-\frac{E_A}{kT_s}} - \operatorname{erf}\left(\sqrt{\frac{E_A}{kT_s}}\right)$$

If F is small, the negative surface velocities may be neglected, and P_s can be represented as shown in Fig. 15b. For all cases studied, F is small, e.g., for the argon-argon system $T_s = 13°K$, $E_A/k \geq 120°K$ (Lennard-Jones well-depth), and $F \leq 0.0003$. Thus, negative surface velocities have been neglected for all computer calculations, and P_s has the approximate functional form,

$$P_s \approx \operatorname{erf}\left(\sqrt{\frac{m}{2kT_s}}\, V_n\right) \quad V_n \geq 0$$

The value of P_s is randomly selected, and the corresponding argument of the error function is determined. The calculated value of the micronormal velocity of the surface atom is then exchanged with the corresponding component of the incident ray.

3.2.2 Spatial Distributions and Capture Coefficients

The in-plane normalized spatial distributions for various surface temperatures are shown in Fig. 16 for a 70-deg incident beam. It is observed that the inclusion of surface temperature in the model tends to broaden the reflected distributions. The in-plane scattering is significantly increased when the surface temperature is raised from 0°K to 13.5 and 23°K.

A numerical test case was run for a 0.50-ev beam incident at 70 deg upon a 13.5°K surface with an attractive field energy of $E_A/k = 467°K$. The capture coefficient for this case was 0.28 as compared with 0.68 for conditions which were identical with the exception that $T_s = 0°K$. Thus, the beam capture coefficient is a strong function of the surface temperature.

Normalized distributions for test cases at various incidence angles and $E_A/k = 467°K$ are presented in Fig. 17. It may be concluded that the shape of these in-plane distributions are independent of the angle of incidence. Also, comparing the in-plane distributions with their corresponding out-of-plane patterns at $\theta_r = \theta_{rm}$ (Fig. 18), one observes that the out-of-plane distributions are broader than those in-plane. As the angle of incidence decreases, the transverse lobal plane distributions become broader.

3.3 SUMMARY OF THE PHYSICAL HARD SPHERE MODEL

A hard sphere model with an attractive surface field energy and surface temperature has been formulated in Sections II and III. The model has a single adjustable parameter, i.e., E_A, the attractive surface field energy. From the arguments of Section 3.1.2, one concludes that a calculation of E_A would be highly presumptuous because of the simplicity of the theoretical formulation. Also, negative surface velocities in the micronormal direction have been neglected based on the low probability of their occurrence. The theoretical model will be tested in Section IV by comparison with the experimental data of Busby and Brown (Ref. 14) for the argon-argon gas-surface system. Since a very simple theoretical model has been used to describe a very complex interaction phenomenon, only qualitative agreement with the experimental results should be anticipated.

SECTION IV
COMPARISON WITH EXPERIMENTAL DATA

4.1 THE BEAM CAPTURE COEFFICIENT

As previously stated in Section 3.1.1, the theoretical beam capture coefficient is defined as the ratio of the number of rays captured to the total number of incident rays, whereas its experimental value is determined as described in Ref. 14. The experimental beam capture coefficient was defined as

$$C_b = 1 - \dot{n}_r/\dot{n}_i$$

where $\dot{n}_r$ is the total reflected flux and $\dot{n}_i$ is the total incident flux. The reflected beam flux is the difference between the total gas flux leaving the surface and the evaporation flux. In the experiments, the evaporation flux was not detectable. Since the evaporation flux can be neglected over the experimental range of conditions, the definition of the experimental and theoretical beam capture coefficients are equivalent. A comparison of the experimental and theoretical beam capture coefficients will be made as the beam incidence angle, beam energy, and surface temperature are varied.

4.1.1 Variation of Beam Incidence Angle

The experimentally measured beam capture coefficients and their corresponding theoretically determined values for various angles of incidence are shown in Fig. 19. Both the theoretical and experimental capture coefficients are monotonically decreasing functions as the angle of incidence increases for E_i = 0.50, 0.43, 0.37, and 0.30 ev.

The magnitude of the attractive surface field energy, E_A/k, was selected to be 590°K for the theoretical calculations since this value gave satisfactory agreement between theory and experiment. However, one cannot with confidence place a great deal of physical significance on the selected value of E_A because of the extreme simplicity of the model. Nevertheless, it is observed in this and succeeding sections that, once the theoretical value of E_A is fixed (E_A/k = 590°K for the argon-argon system at T_s = 13.5°K), the agreement between theory and experiment is consistent in at least three ways: (1) capture coefficients for various incidence angles (Section 4.1.1), (2) capture coefficients for various beam energies (Section 4.1.2), and (3) spatial distributions (Section 4.2). This consistency gives credence to the model even though the absolute physical value of E_A is unknown.

4.1.2 Variation of Beam Incident Energy

A comparison of the theoretical and experimental beam capture coefficients for various incidence energies is presented in Fig. 20. The coefficients are monotonically decreasing functions as the beam incidence energy increases for θ_1 = 30, 45, 60, and 70 deg. The value of E_A/k is still 590°K, and agreement between theory and experiment is consistently good over the range of conditions.

4.1.3 Variation of Surface Temperature

Since it is assumed that the surface field energy is related to the heat of sublimation, the value of E_A changes as the surface temperature is varied. The equilibrium value of the heat of sublimation, H_s, for argon was shown in Fig. 12 as T_s increases. Although the molecular beam-solid surface interaction is a nonequilibrium process, H_s still increases as T_s increases over the experimental surface temperature range from 13 to 23°K.

A comparison of the experimental and theoretical capture coefficients as surface temperature varies is shown in Fig. 21. Values of E_A were selected such that close agreement between the measured and calculated values was obtained. A comparison of H_s

and E_A, normalized by their values at 13°K, for various surface temperatures, is presented in Fig. 22. These empirical values are larger than the equilibrium values. There are at least three possible explanations for this discrepancy:

1. The experimental data could be in error. The surface temperature experiments were the most difficult to perform because of the problem of maintaining the target at a constant temperature.

2. The heat of sublimation into a vacuum is somewhat higher than the equilibrium value. Although the value of H_s would increase as T_s increases, it is not of such magnitude as to account for the corresponding values of E_A.

3. It is possible that the comparatively large values of E_A result from second-order effects which may become important at higher surface temperatures such as the shape of the potential function, etc. Such effects are not and cannot be included in the model.

4.2 THE SPATIAL DISTRIBUTIONS

The theoretical and experimental data presented in this section are representative samples chosen to show the effects of varying beam incidence angle and energy on the reflected spatial distributions. A comparison between the experimental and theoretical in-plane scattering patterns is shown in Figs. 23 through 27 for various beam incidence conditions.

An increase in scatter in the theoretical data is observed as the incidence angle and energy decrease. This is due to the increase in the capture coefficient; i.e., the number of rays in a particular spatial distribution cell decreases as the probability of capture increases, and the theoretical distributions will be less smooth because of the decrease in the number of samples. Nevertheless, the theoretical trends are evident, and the large increase in computer time necessary to produce smooth distributions was not considered justifiable.

Both the theoretical and experimental in-plane spatial distribution lobes have maxima at approximately 75 deg. However, in all cases the theoretical distributions are much more narrow than their corresponding experimental lobes. The narrowness may be attributed to the following:

1. The surface is assumed to be planar (Assumption 4), and thus the broadening effects of surface roughness have not been considered. The structure of the surface is the largest experimental unknown (Ref. 14), and thus no estimate of the magnitude of the surface roughness can be confidently made. Also, the inclusion of surface roughness in the model would inordinately increase the computation time.

2. The finite width of the experimental molecular beam has not been included in the model. The theoretical distributions are the result of scattering from an area the size of a single surface module.

3. The change in the radius of the module spherical cap, R (sum of the radii of the initial gas and surface atoms), is not considered. As the energy of the incident gas atom increases, the depth of penetration into the repulsive potential field of the surface atom increases. Thus, the effective value of R decreases as E_i increases, and the surface appears to be rougher to the incident ray thus broadening the scattering distribution. The concept of an effective radius as a function of gas energy for a hard sphere model was proposed by Sutherland (Ref. 15) in 1893. However, his theory can only be properly applied for the collisions of free gas atoms.

Computational difficulties arise in the model if a variable R is included. Rays undergoing multiple collisions are partially accommodated, i.e., R changes during each collision, and this would give rise to geometrical computational problems.

Thus, these three effects would tend to broaden the scattering distributions. Their effects are only mentioned and not included since the model would become unjustifiably complicated, i.e., other adjustable parameters would have to be included and the comparison between theory and experiment would become an exercise in curve fitting.

SECTION V
CONCLUSIONS

A classical theoretical model for gas-surface interaction has been formulated and compared with the experimental data for the gaseous-argon solid-argon system. The theoretical interaction was modeled as basically the collision of hard spheres with the inclusion of surface temperature and an attractive surface field energy. The model has a single adjustable parameter, E_A. However, when a value of E_A is chosen, it remains fixed for all beam incidence conditions. The model does not include the physical conditions of surface roughness, finite beam width, and a variable depth of penetration into the repulsive potential field of the surface atoms.

Surprisingly, the theoretical results from this exceedingly simple model exhibit nearly every characteristic of the experimental observations. These characteristics may be summarized as follows:

1. The angle of maximum reflected intensity for both theory and experiment was independent of the beam incidence angles, incident energies, and surface temperatures studied and was approximately equal to 75 deg (Section 4.2).

2. The experimental and theoretical beam capture coefficients are monotonically decreasing functions as the beam incidence angle or energy increases (Sections 4.1.1 and 4.1.2).

3. The shapes of the normalized in-plane spatial distributions are independent of the angle of incidence (Section 3.2.2).

4. The out-of-plane spatial distributions are broader than their corresponding in-plane patterns (Section 3.2.2).

Since the theoretical model can be used consistently to qualitatively describe the experimental data, several general conclusions can be reached concerning the actual physical gas-surface interaction:

1. Classical mechanics appears to be a sufficient level of description for the interaction of a monatomic gas with its own solid phase. Quantum effects seem to be at least of second order.

2. A hard sphere model is adequate to predict the gas-solid collision properties in the range of the experimental conditions although the theoretical spatial distributions are narrower than those experimentally measured.

3. The experimental results indicated that energy transfer between the incident atoms and surface was very efficient, e.g., at $\theta_i = 0$ deg and $E_i = 0.50$ ev, the capture coefficient was greater than 0.99. This fact required the selection of a significantly higher value of the attractive surface field energy (the basis for the theoretical capture criterion) than has been used for other gas-surface systems (Refs. 1, 6, 8, and 9). However, this value was still within the physical limits of the gas-surface system under study (Section 3.1.3). Nevertheless, it must be emphasized that the theoretically determined value of E_A is probably a strong function of the model used to describe the interaction but should not be interpreted as the absolute physical value of the surface field energy.

When more complete experimental results are obtained, in particular, energy and momentum accommodation measurements, the validity of the present model may be tested even further.

REFERENCES

1. Goodman, F. O. "Three Dimensional Hard Spheres Theory of Scattering of Gas Atoms from a Solid Surface. I. Limit of Large Incident Speeds." Surface Science, Vol. 7, July 1967. pp. 391–421.

2. Baule, B. "Theoretische Behandlung der Ersheinungen in Verdunnten Gasen." Annalen der Physik, Vol. 44, 1914. pp. 145–176.

3. Oman, R. A., Bogan, A., Weiser, C., and Li, C. H. "Interactions of Gas Molecules with an Ideal Crystal Surface." AIAA Journal, Vol. 2, No. 10, October 1964. pp. 1722–1730.

4. Oman, R. A. "Research in Gas-Surface Interactions. 1964-65. Part I. Numerical Calculations of Gas-Surface Interactions." Grumman Research Report RE-222, 1965.

5. Oman, R. A., Calia, V. S., and Weiser, C. H. "Research on Gas-Surface Interactions 1965-66." Grumman Research Report RE-272, 1966.

6. Logan, R. M., Keck, J. E., and Stickney, R. E. "Simple Classical Model for the Scattering of Gas Atoms from a Solid Surface II. Additional Analyses and Comparisons." Proceeding 5th International Symposium Rarefied Gas Dynamics, Academic Press, New York. Vol. 1, 1966. pp. 259–261.

7. Logan, R. M. and Stickney, R. E. "Simple Classical Model for the Scattering of Gas Atoms from a Solid Surface." Journal Chemical Physics, Vol. 44, No. 1, January 1966. pp. 195–201.

8. Jackson, D. P. "A Theory of Gas-Surface Interactions at Satellite Velocities." UTIAS Report No. 134, November 1968.

9. Goodman, F. O. "On the Trapping Process in Gas-Surface Interactions." Rarefied Gas Dynamics, 6th Symposium ed. L. Trilling and N. Y. Wachman, Academic Press, New York, Vol. 2, 1969. pp. 1105–1118.

10. Young, D. M. and Crowell, A. D. Physical Adsorption of Gases. Butterworths, London, 1962. p. 11.

11. Hirschfelder, J. O., Curtiss, C. F., and Bird, R. B. Molecular Theory of Gases and Liquids. John Wiley and Sons, Inc., New York, 1954. p. 168.

12. Ziegler, W. T., Mullins, J. C., and Kirk, B. S. "Calculation of the Vapor Pressure and Heats of Vaporization and Sublimation of Liquids and Solids, Especially below One Atmosphere Pressure. II Argon." Technical Report No. 2, Project Report No. 2, Engineering Experiment Station, Georgia Institute of Technology, Atlanta, Georgia, June 1962.

13. Vincenti, W. G. and Kruger, C. H., Jr. Introduction to Physical Gas Dynamics. John Wiley and Sons, Inc., New York, 1965. p. 48.

14. Busby, M. R. and Brown, R. F. "An Experimental Investigation of the Scattering of a Monoenergetic Argon Molecular Beam from a Solid Argon Surface." AEDC-TR-70-90, July 1970.

15. Sutherland, W. Philosophical Magazine, Series 5, Vol. 36, 1893. p. 507.

APPENDIXES

I. ILLUSTRATIONS

II. TABLE

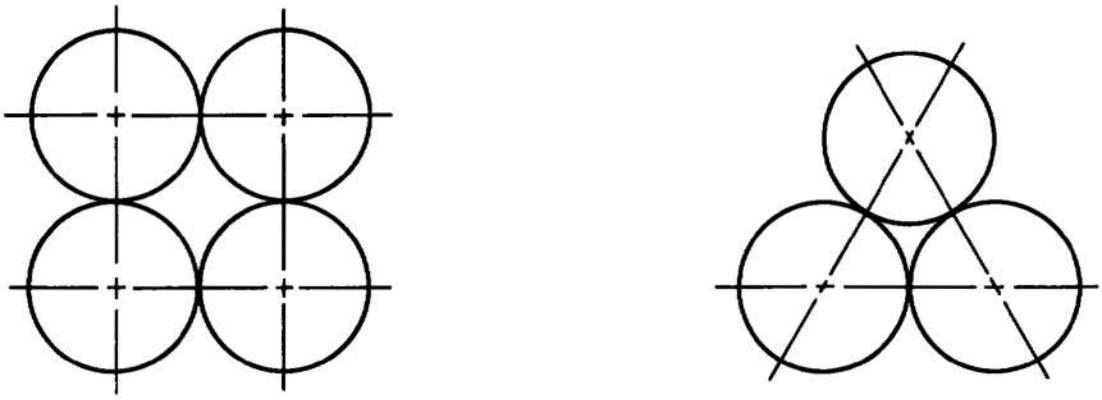

a. Square Array

b. Hexagonal Array

Fig. 1 Surface Configurations

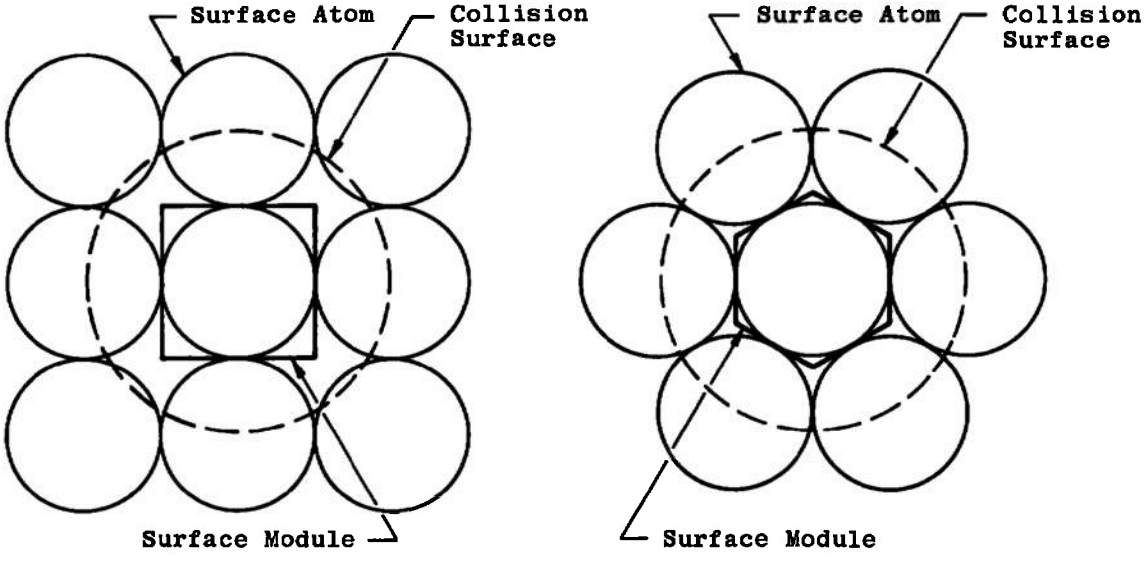

a. Square Surface Array

b. Hexagonal Surface Array

Fig. 2 Relation of Surface Modules to Surface Arrays

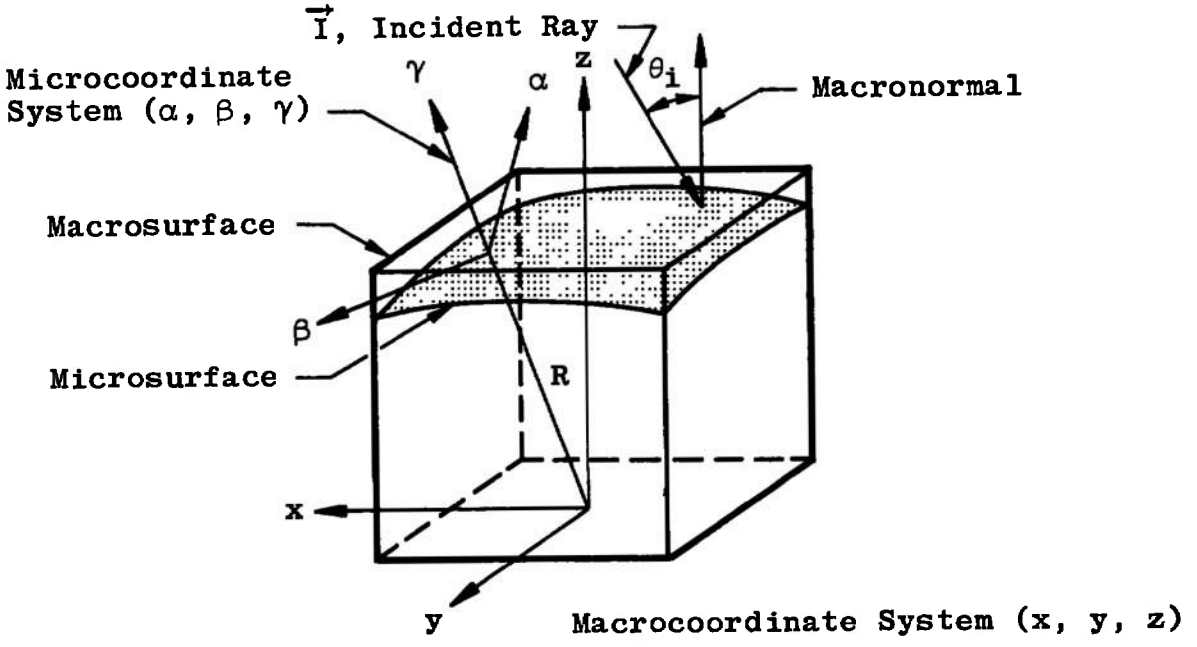

a. Square Module

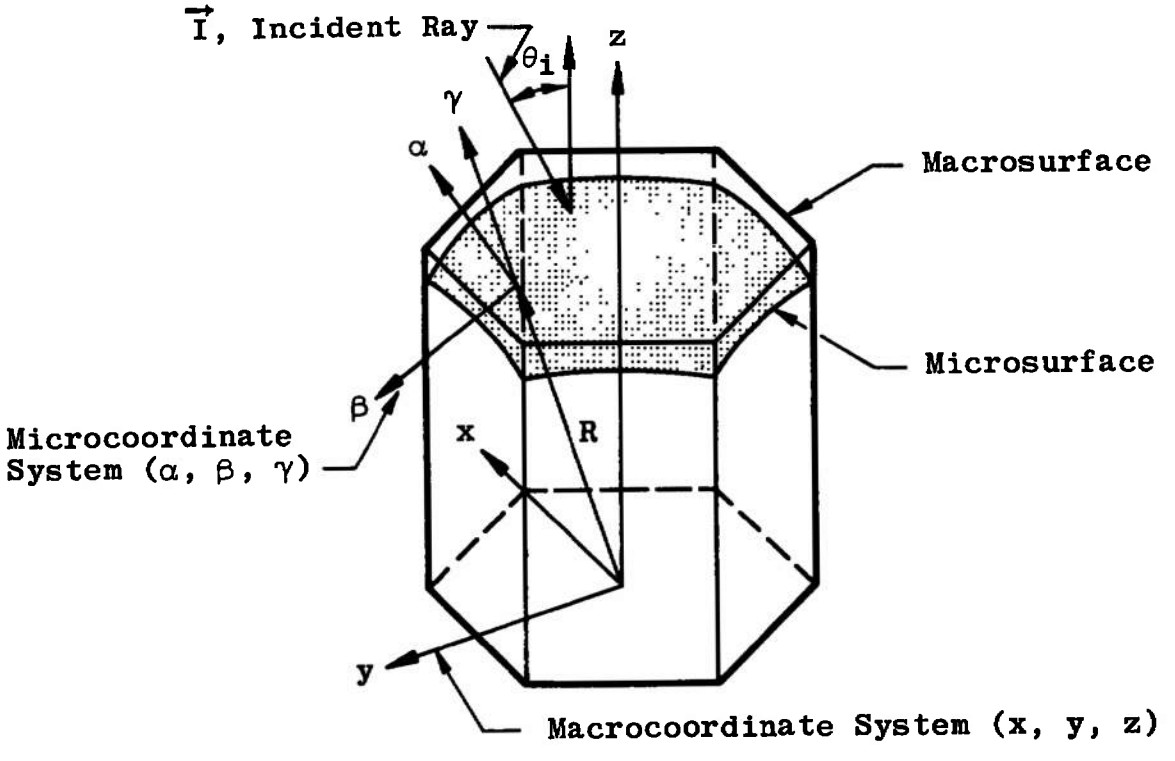

b. Hexagonal Module

Fig. 3 Surface Modules

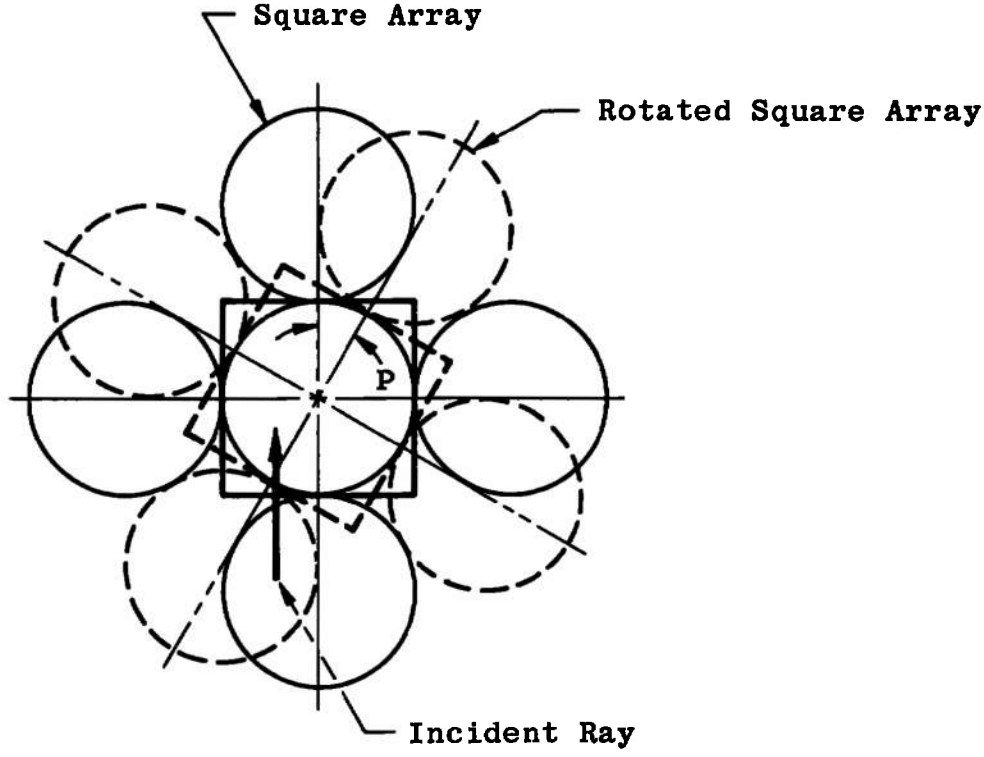

Fig. 4 Randomization of the Surface Module

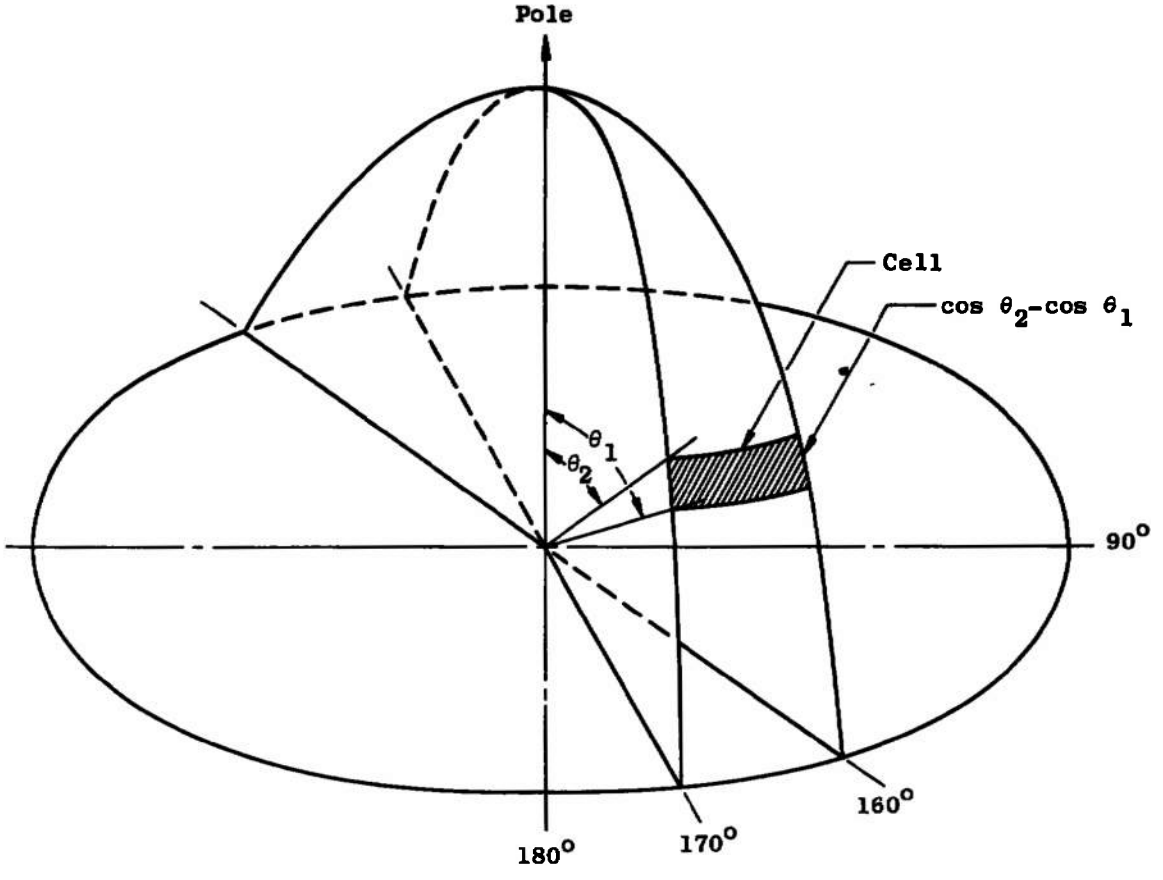

Fig. 5 Normal Polar Directional Map

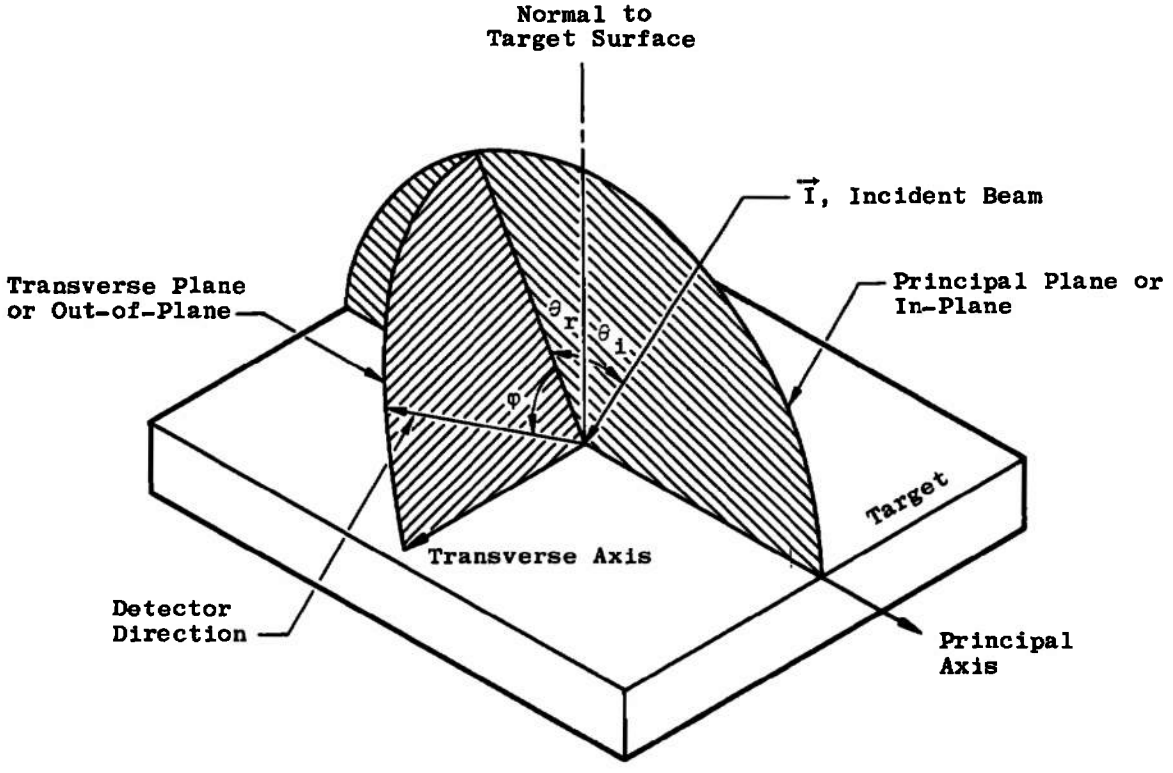

Fig. 6 Orientation Parameters for the Reflected Beam

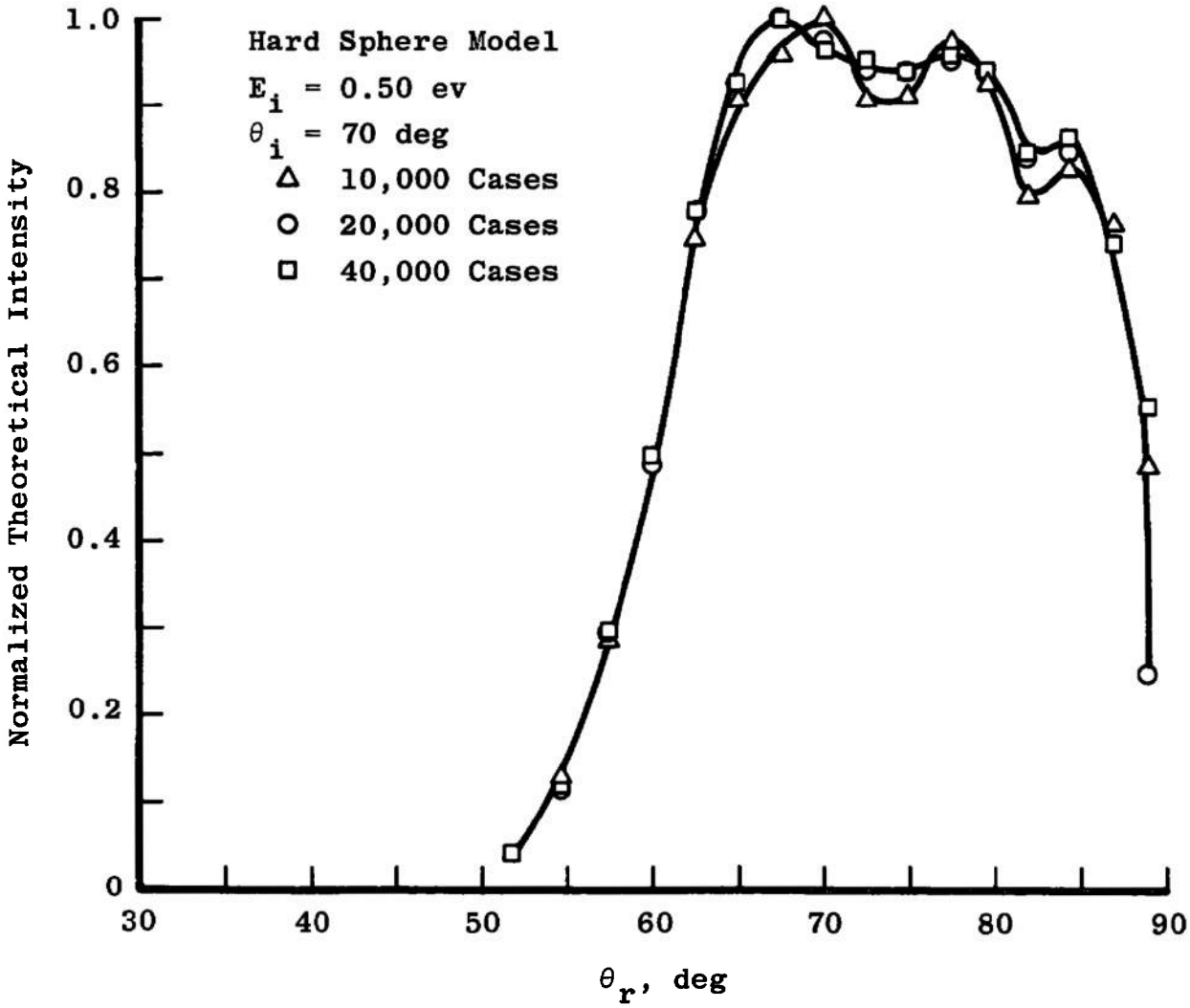

Fig. 7 Variation of the In-Plane Normalized Spatial Distributions with Number of Trajectories

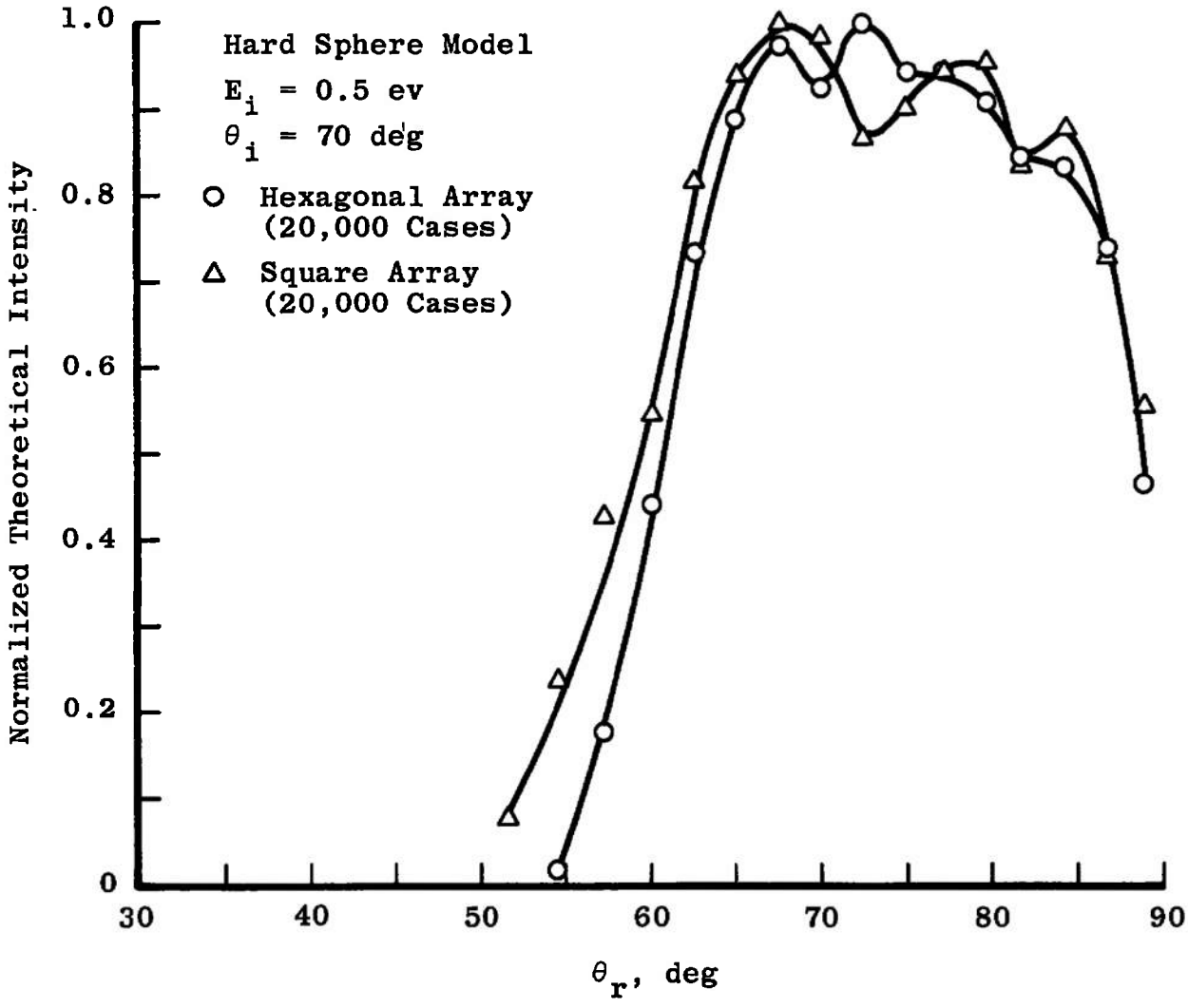

Fig. 8 Comparison of the In-Plane Normalized Spatial Distributions of the Hexagonal and Square Surface Arrays

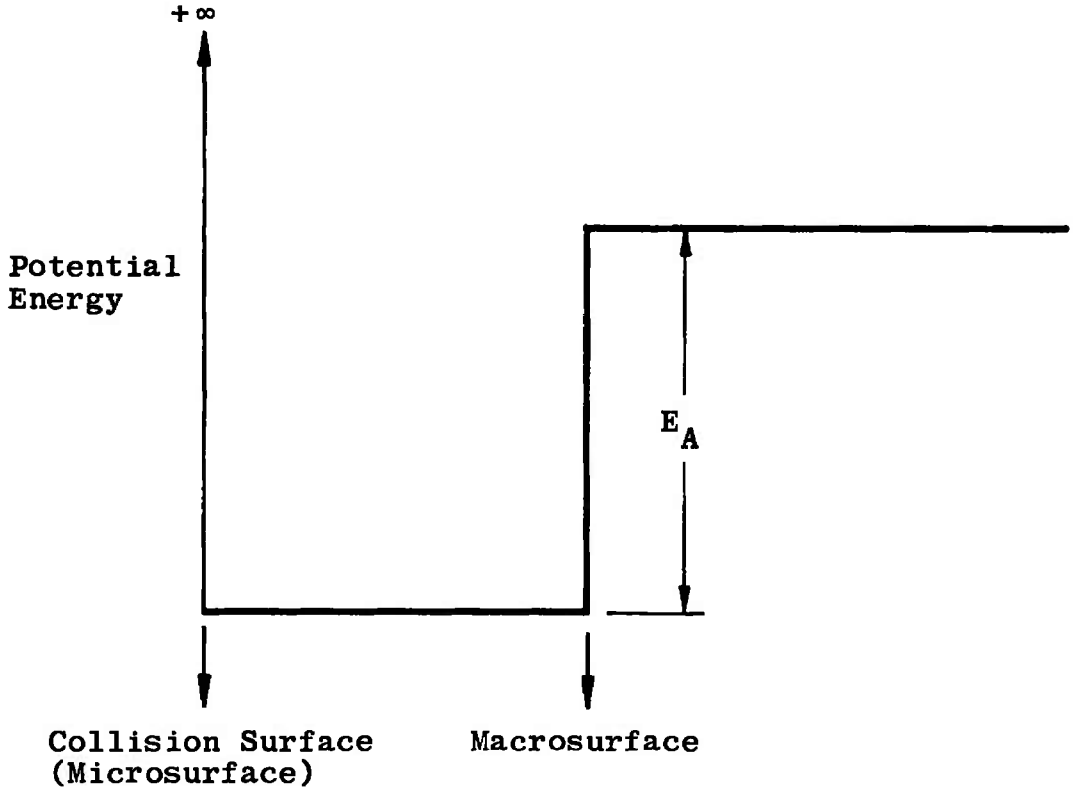

Fig. 9 Square-Well Potential

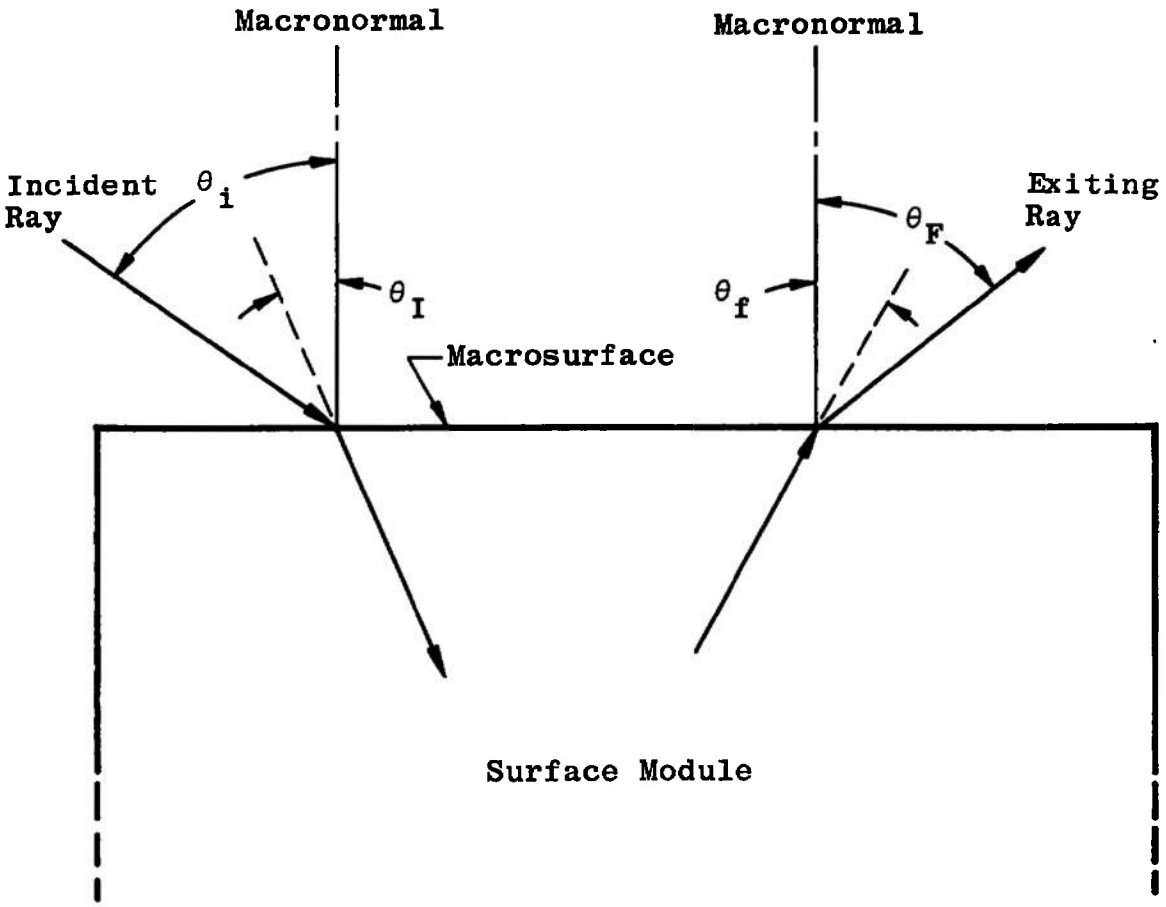

Fig. 10 Trajectory Alterations Due to a Square-Well Potential

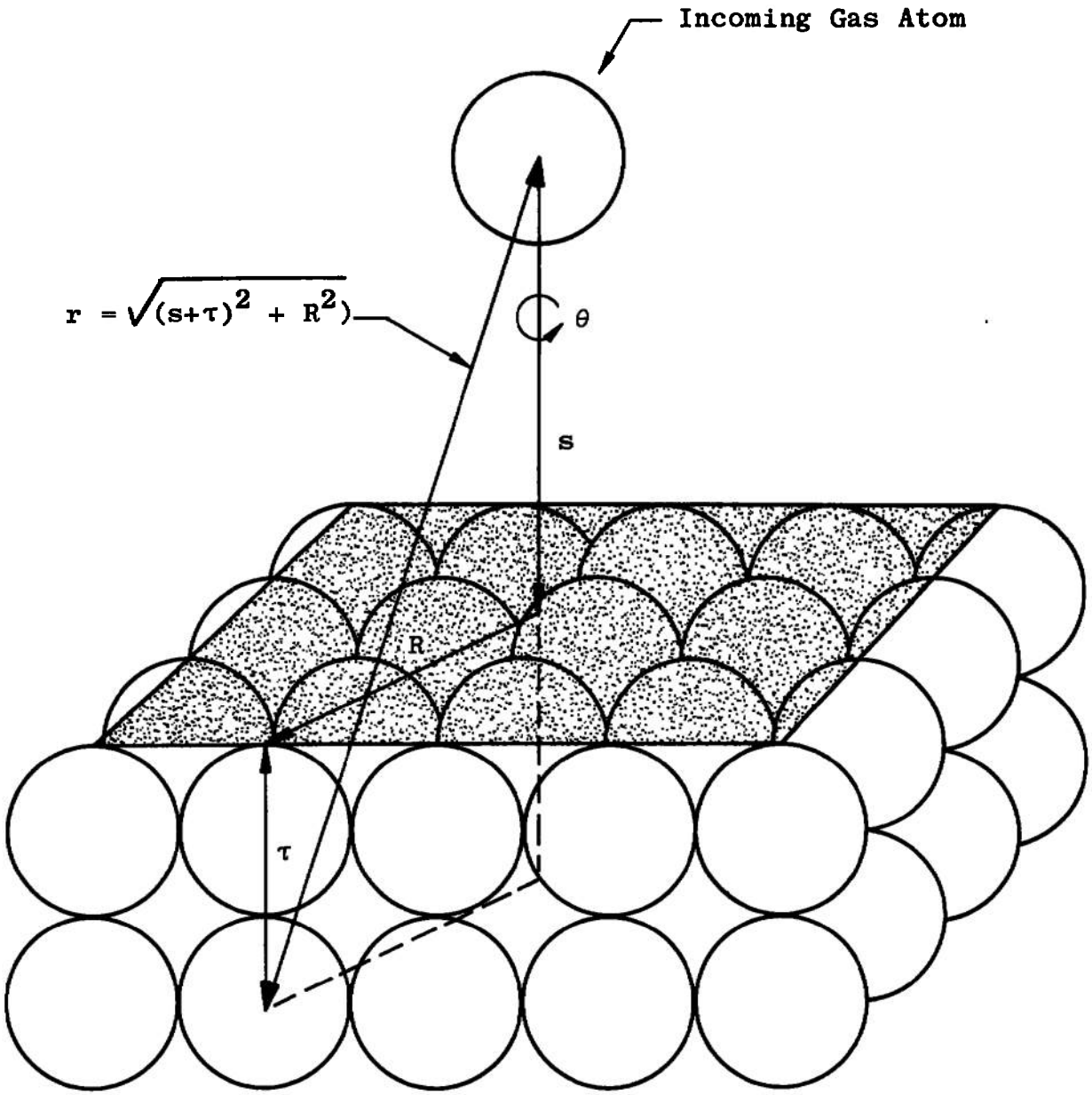

Fig. 11 Geometry for the Estimation of the Surface Field Energy

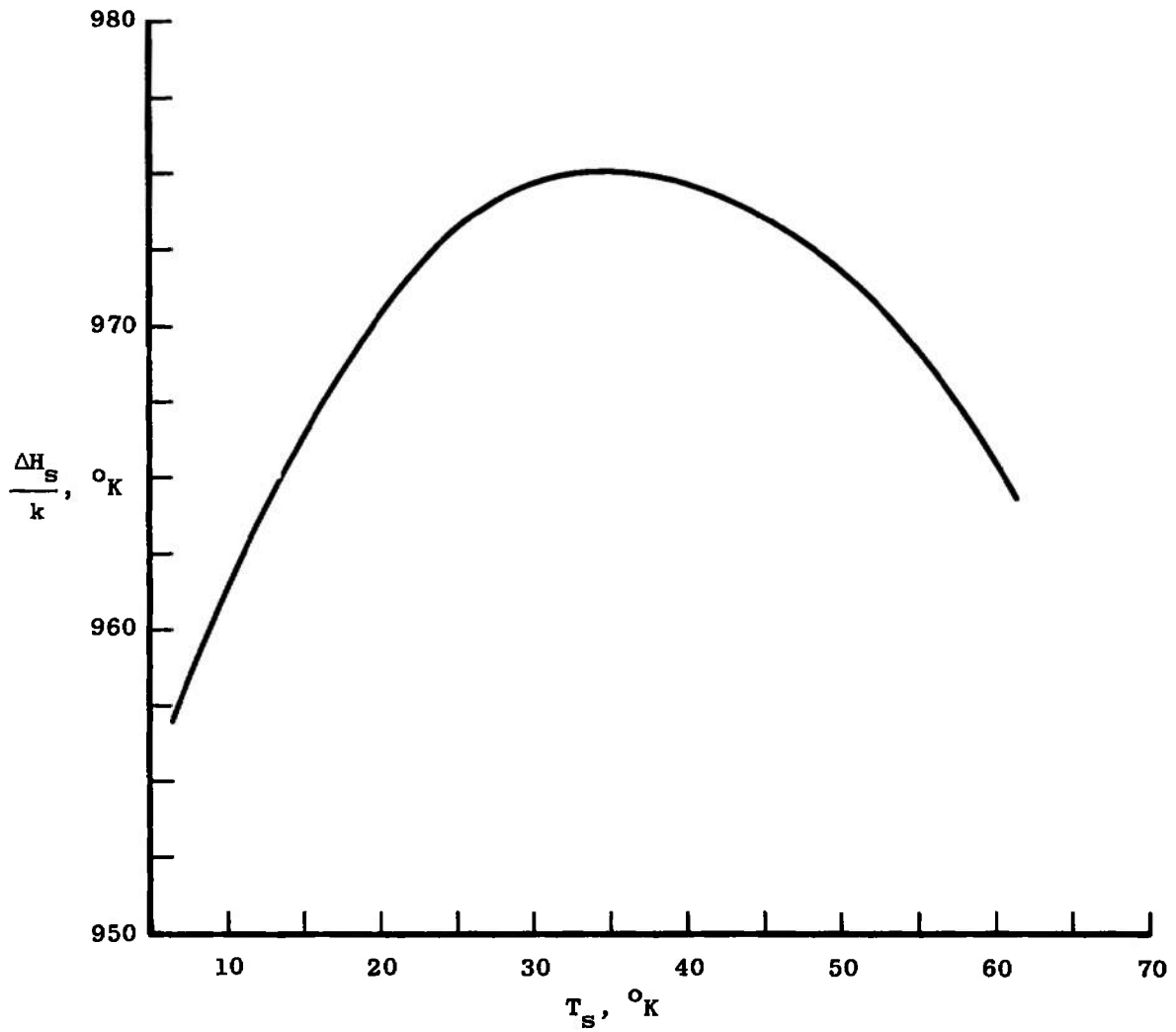

Fig. 12 Heat of Sublimation for Solid Argon at Equilibrium

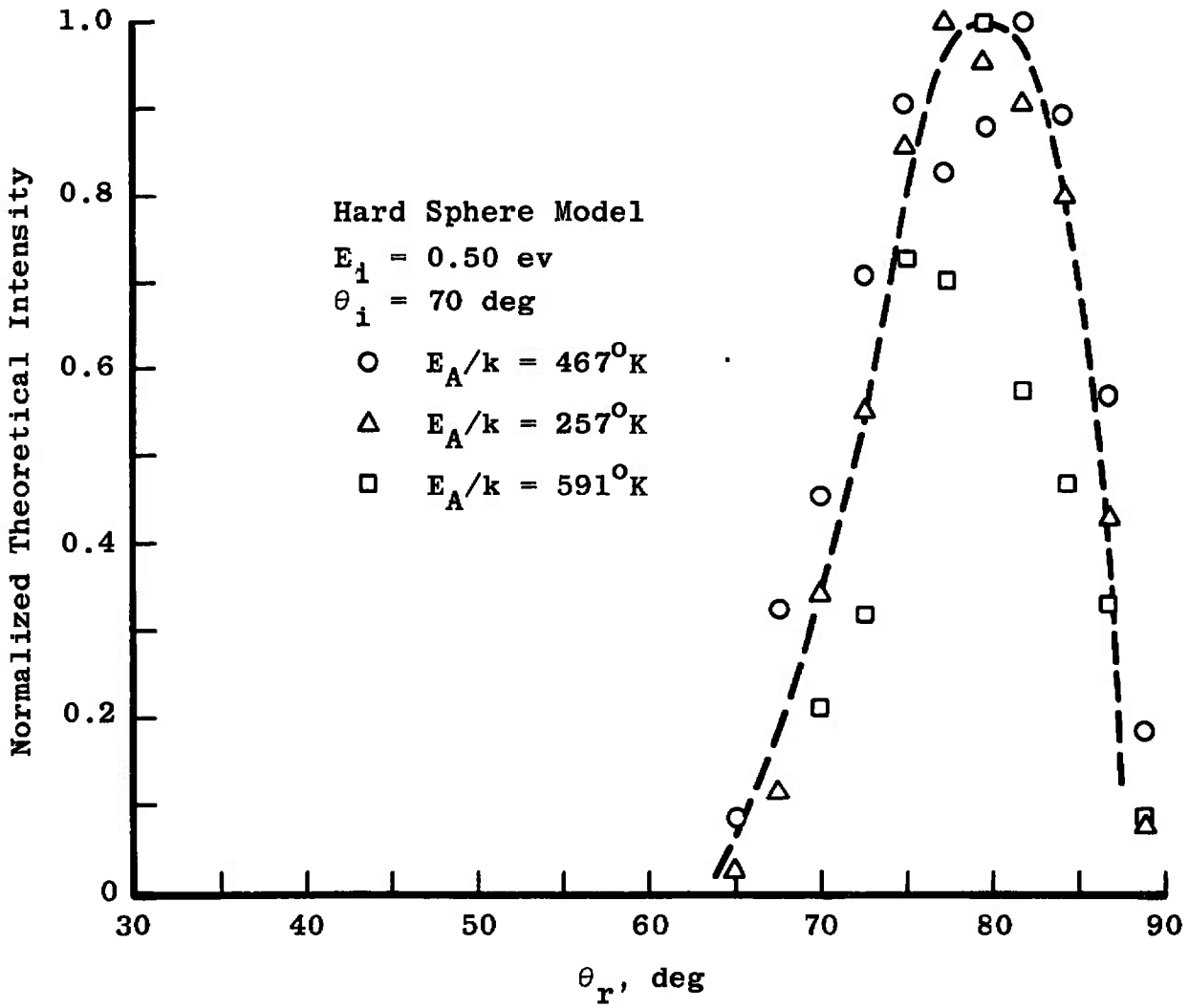

Fig. 13 In-Plane Normalized Spatial Distributions for Various Surface Field Energies

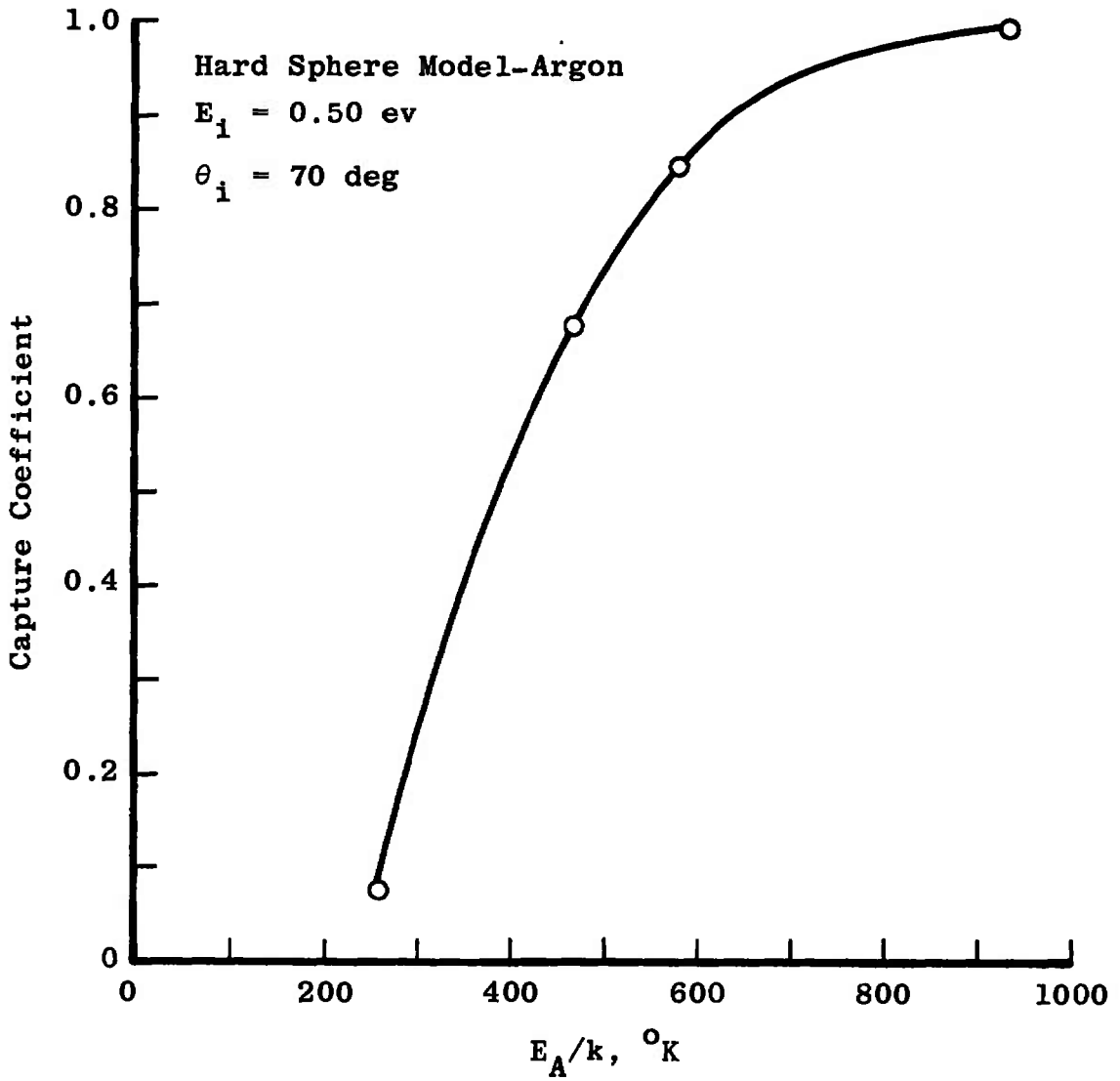

Fig. 14 Beam Capture Coefficient for Various Surface Field Energies

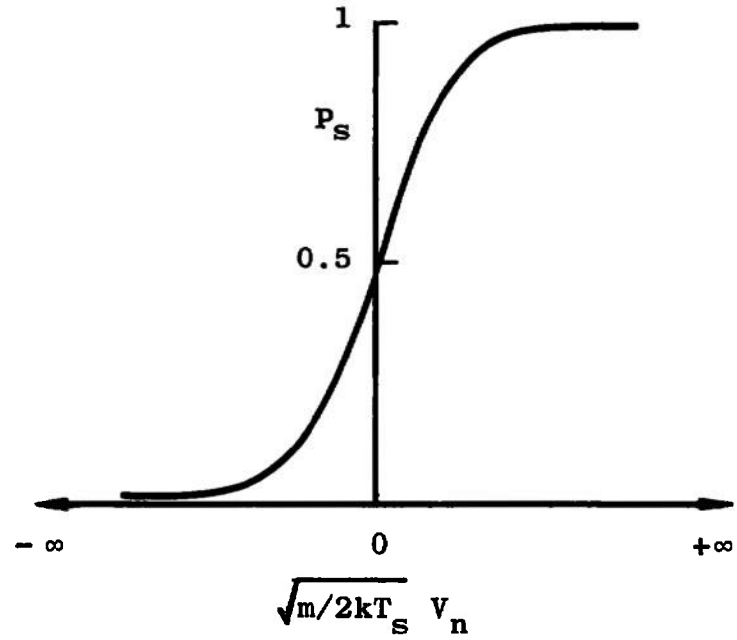

a. P_s for Surface Velocities without an Incident Beam

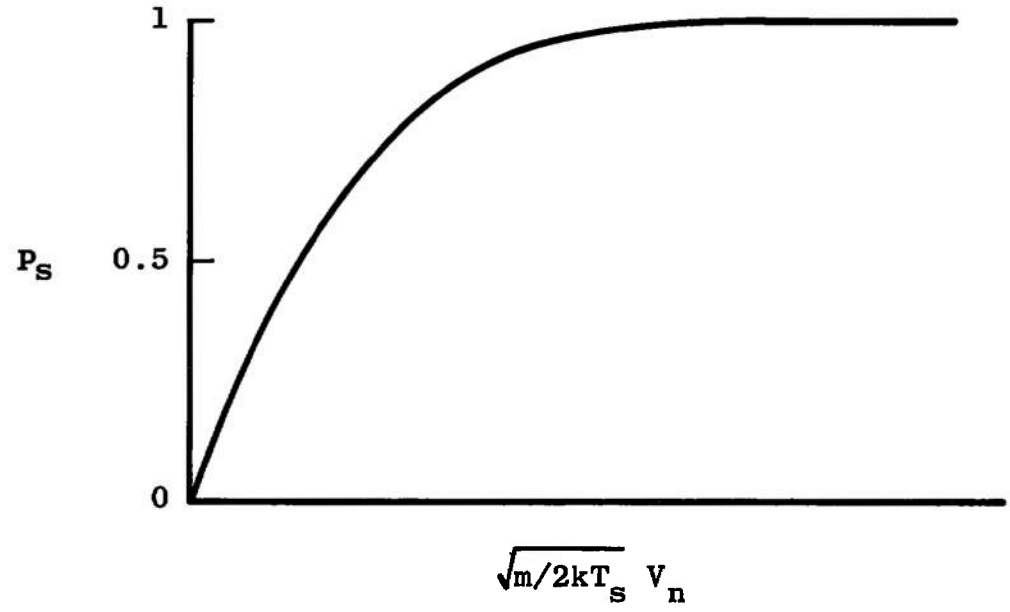

b. P_s for Surface Velocities with an Incident Beam

Fig. 15 Probability for a Surface Velocity

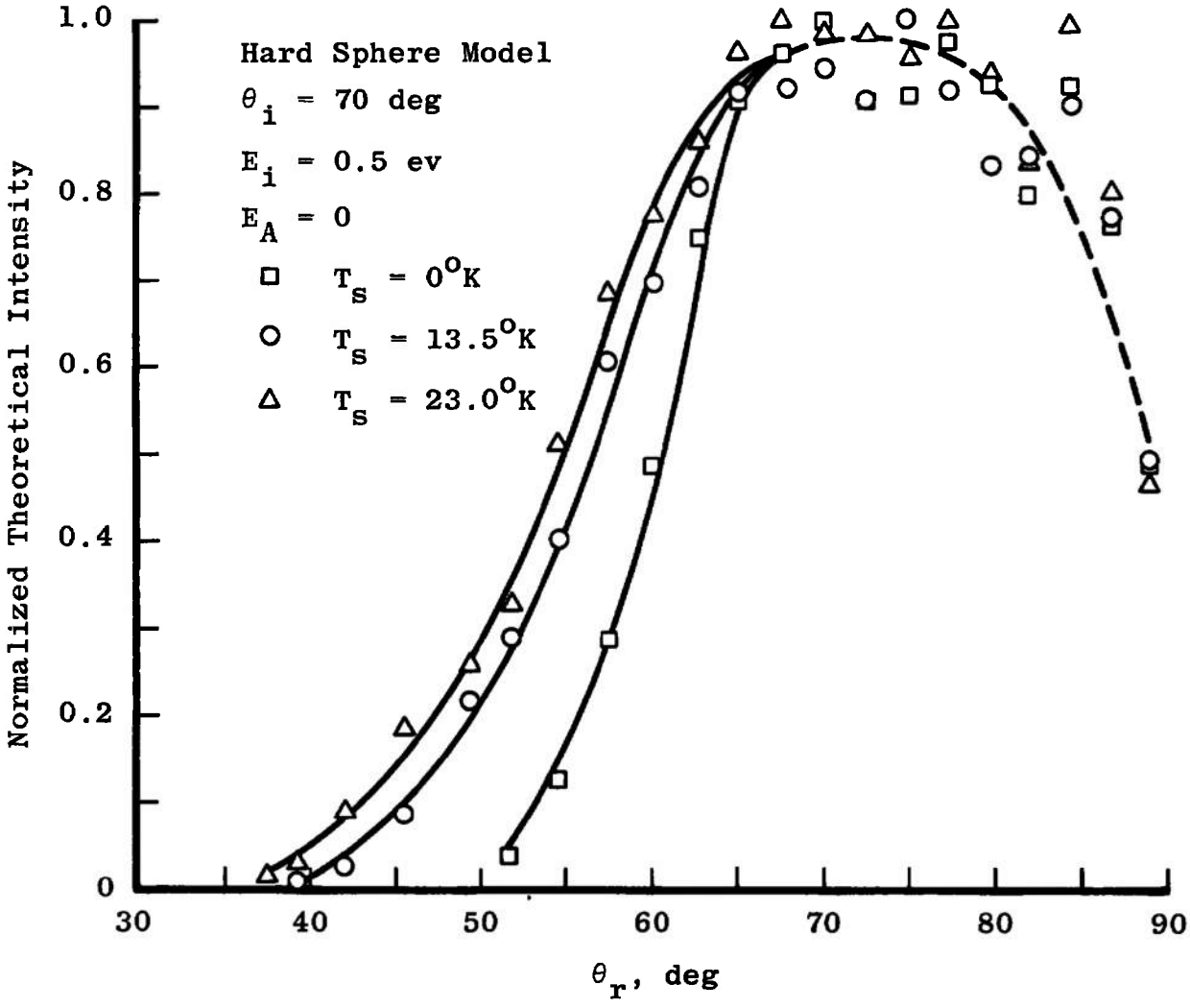

Fig. 16 In-Plane Normalized Spatial Distributions for Various Surface Temperatures

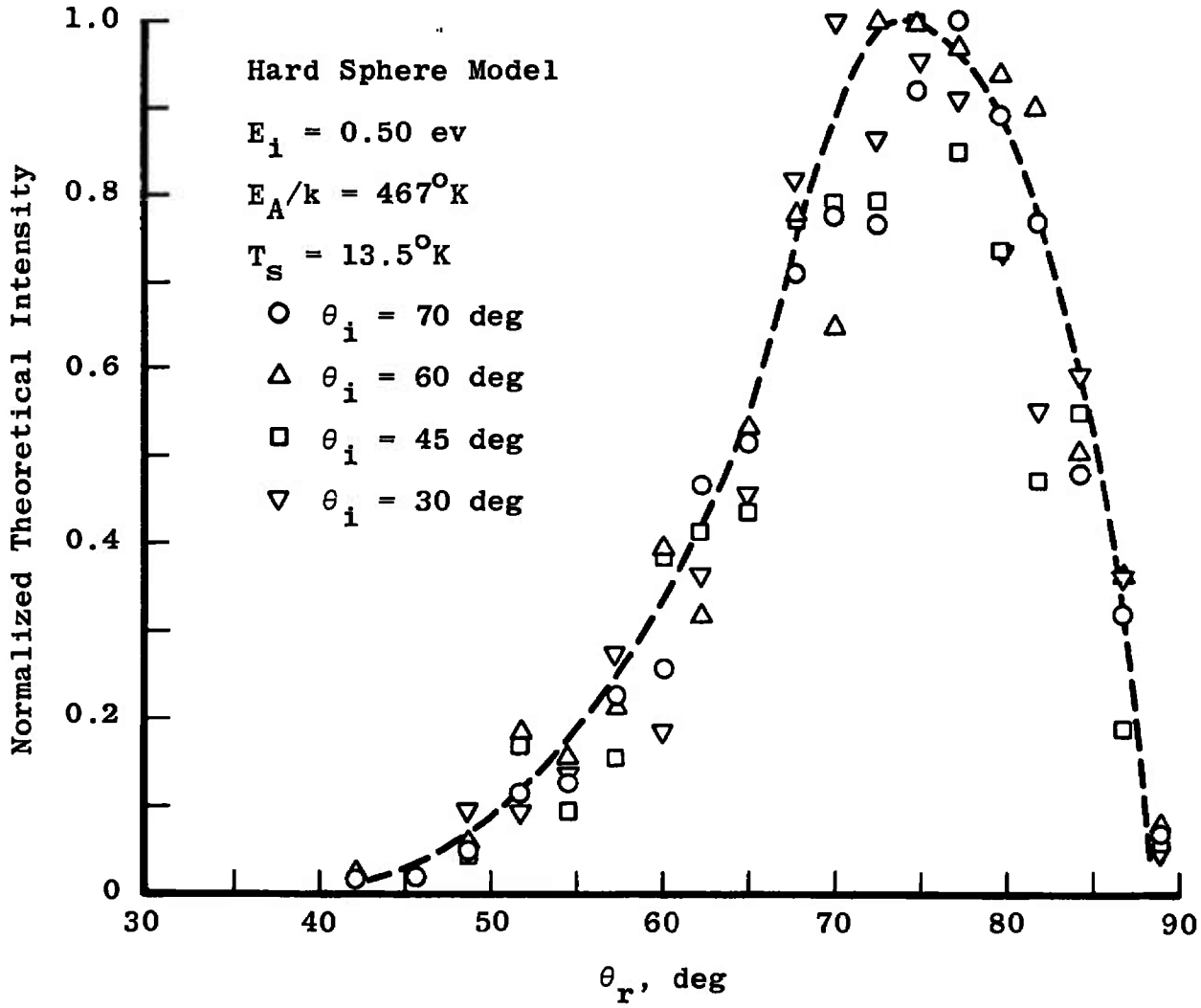

Fig. 17 In-Plane Normalized Spatial Distributions for Various Angles of Incidence

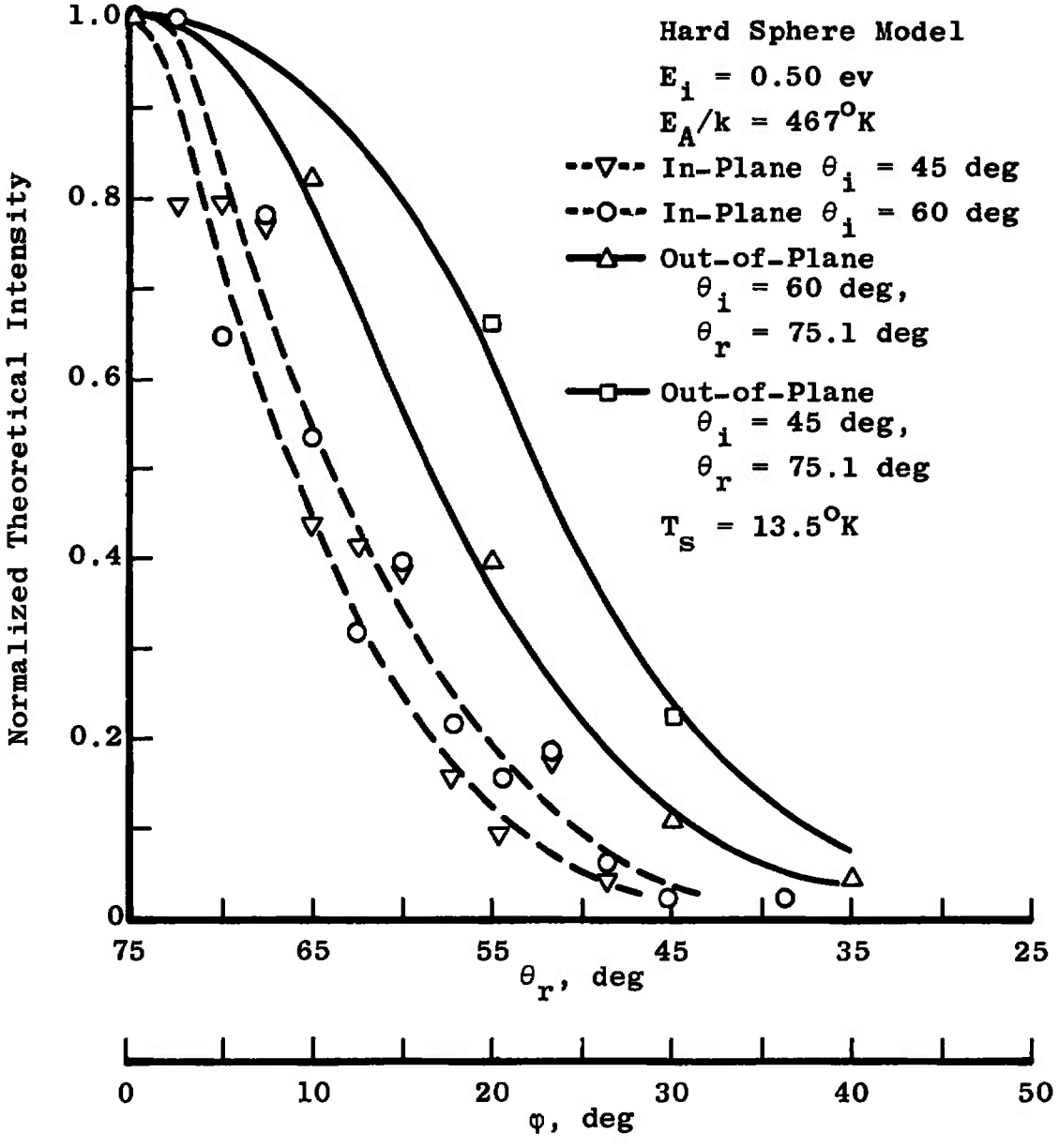

Fig. 18 Comparison of the Normalized In-Plane and Out-of-Plane Spatial Distributions

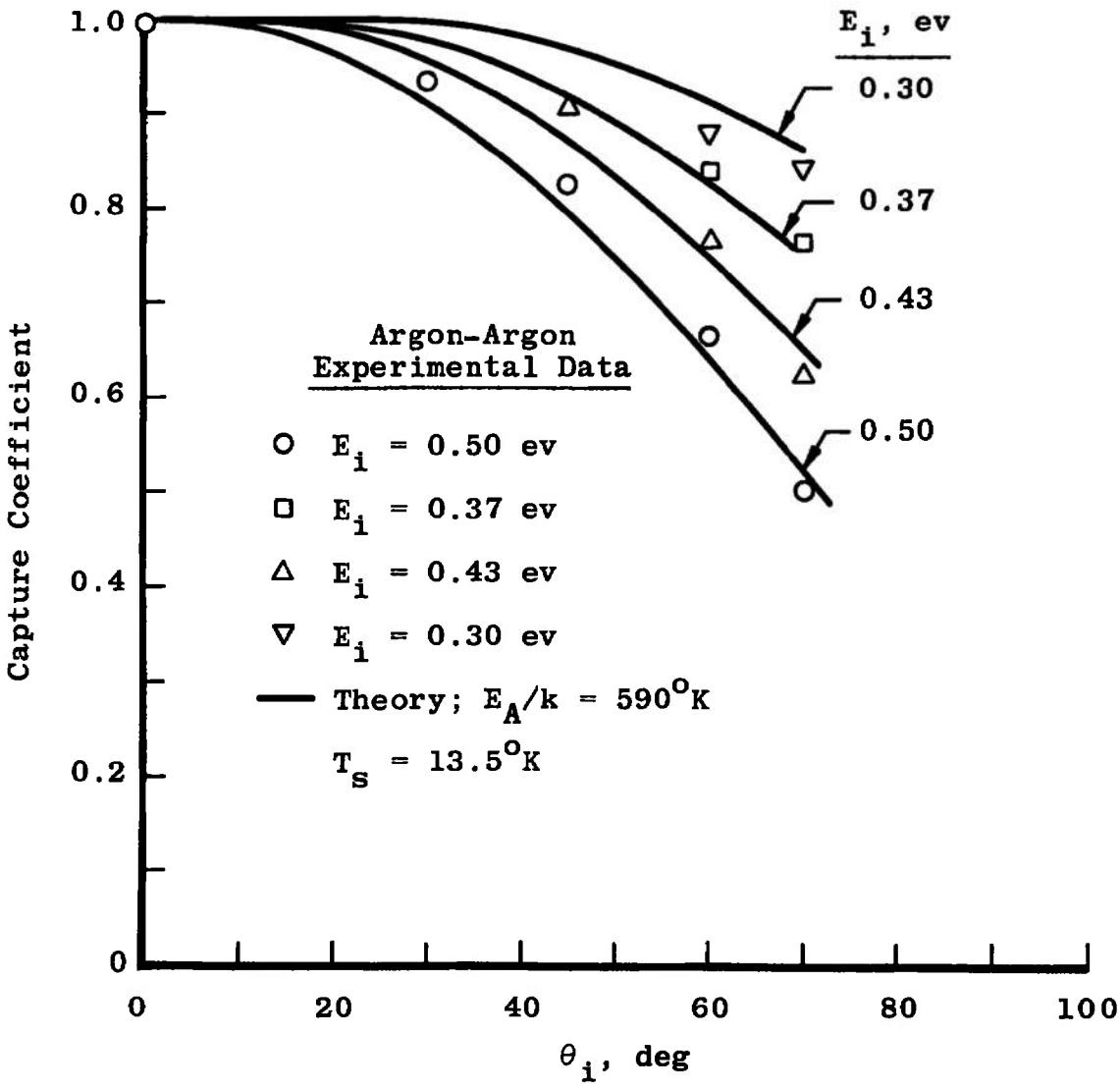

Fig. 19 Beam Capture Coefficient for Various Angles of Incidence—Comparison of Theory and Experiment

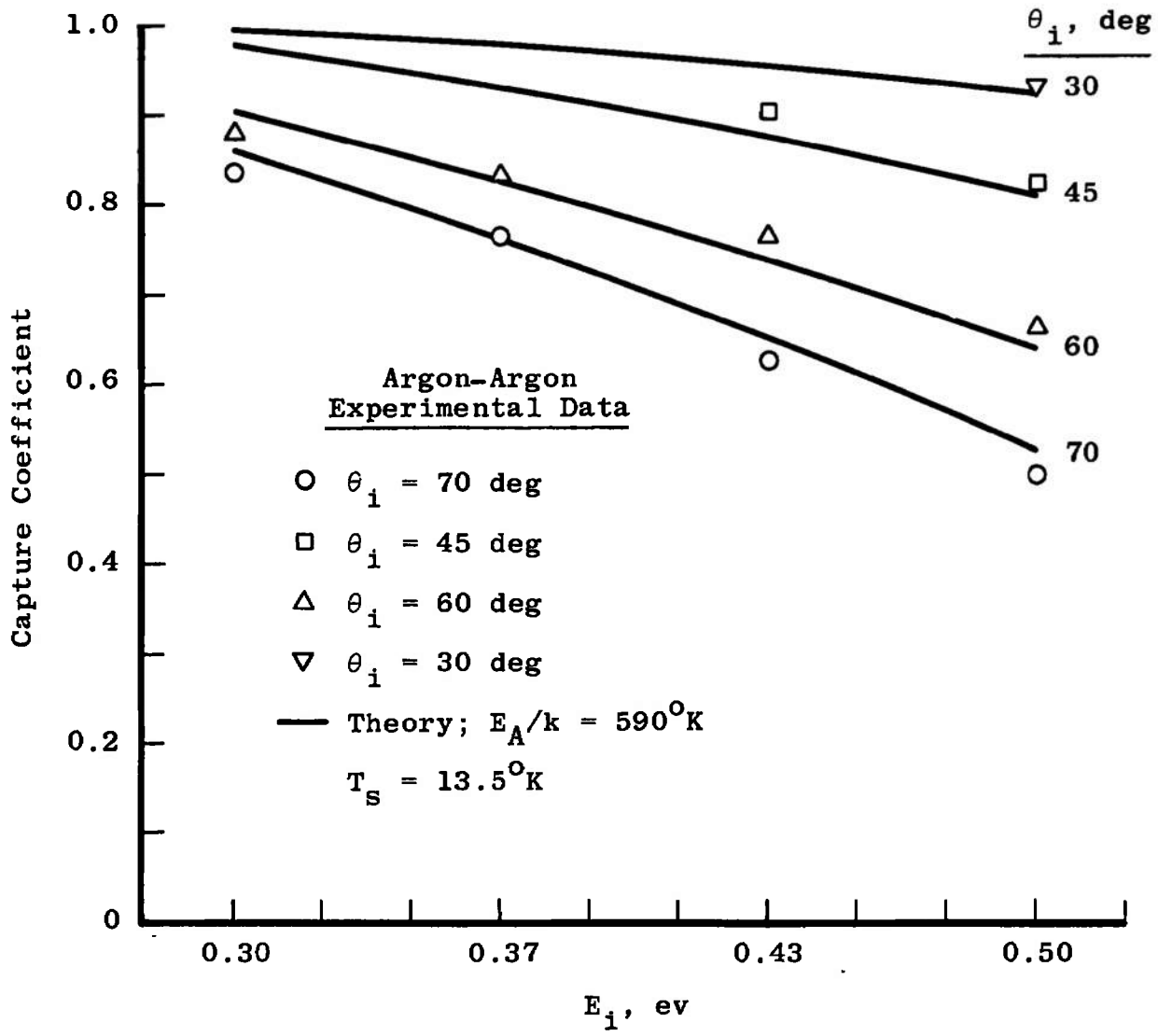

Fig. 20 Beam Capture Coefficient for Various Beam Energies—Comparison of Theory and Experiment

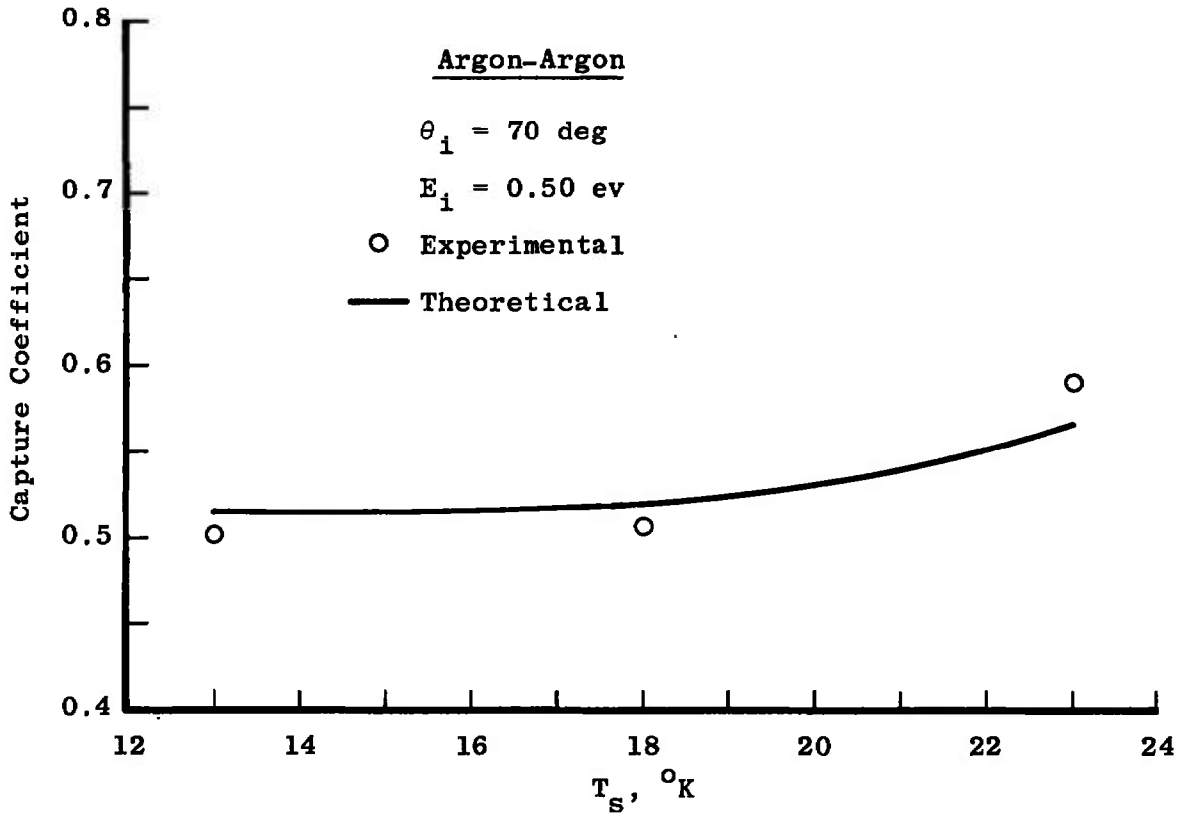

Fig. 21 Beam Capture Coefficient for Various Surface Temperatures—Comparison of Theory and Experiment

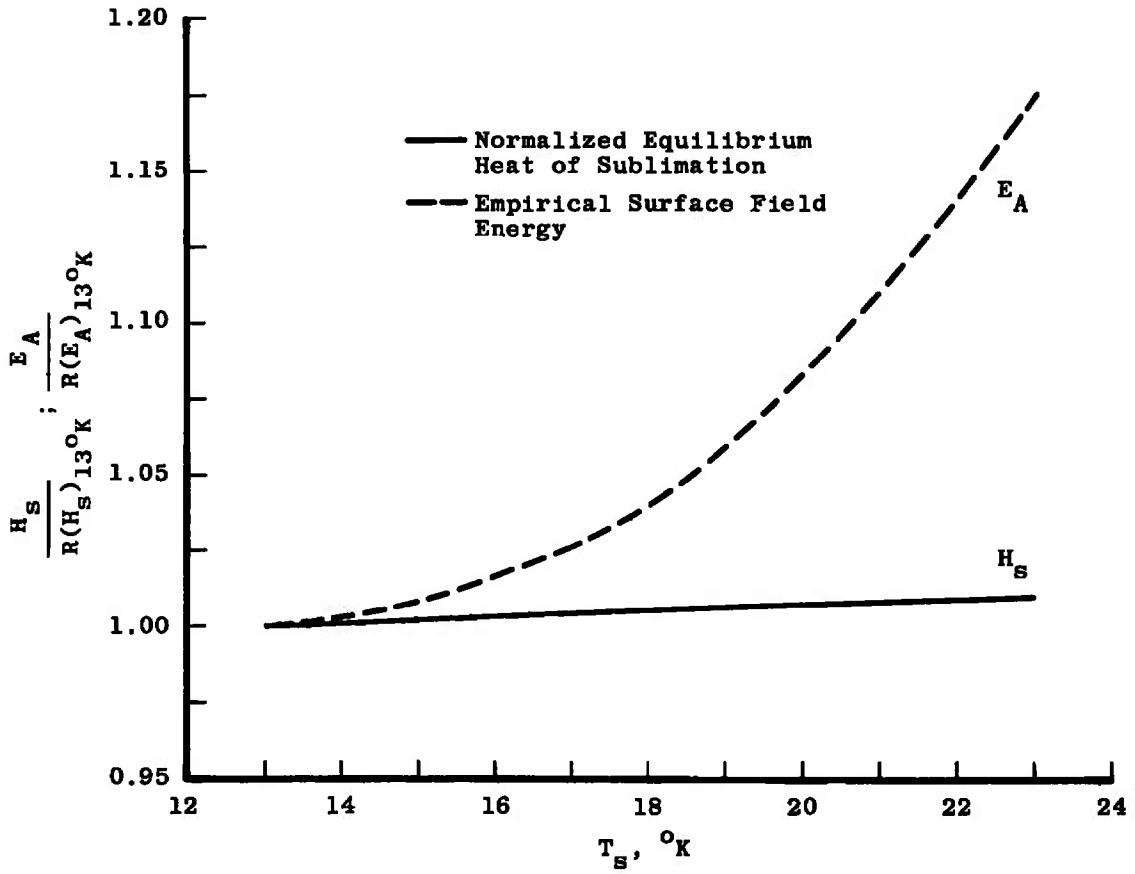

Fig. 22 Comparison of the Normalized Heat of Sublimation and Empirical Attractive Surface Field Energy for Various Surface Temperatures

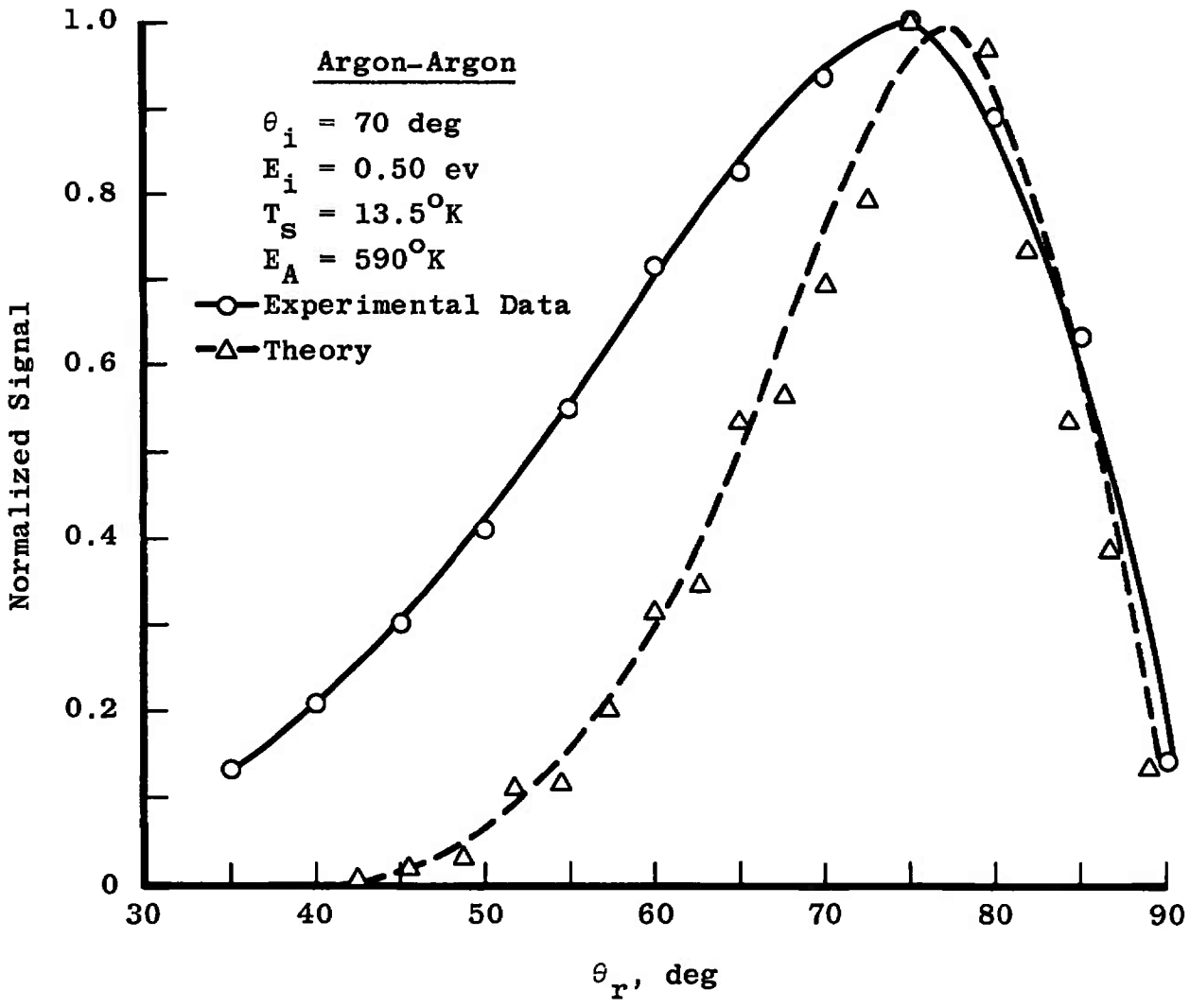

Fig. 23 Normalized In-Plane Spatial Distribution for θ_i = 70 deg and E_i = 0.50 ev

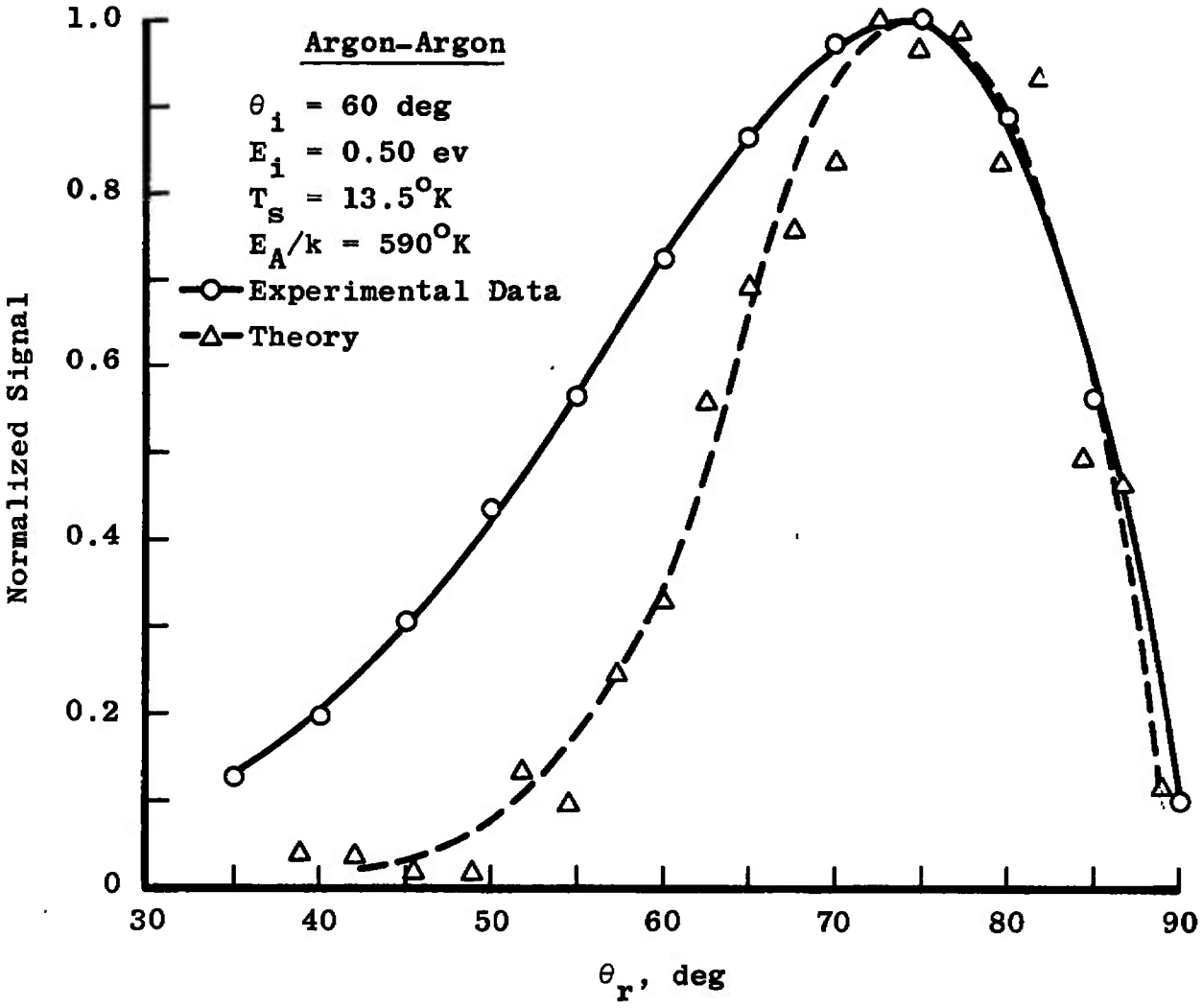

Fig. 24 Normalized In-Plane Spatial Distribution for θ_i = 60 deg and E_i = 0.50 ev

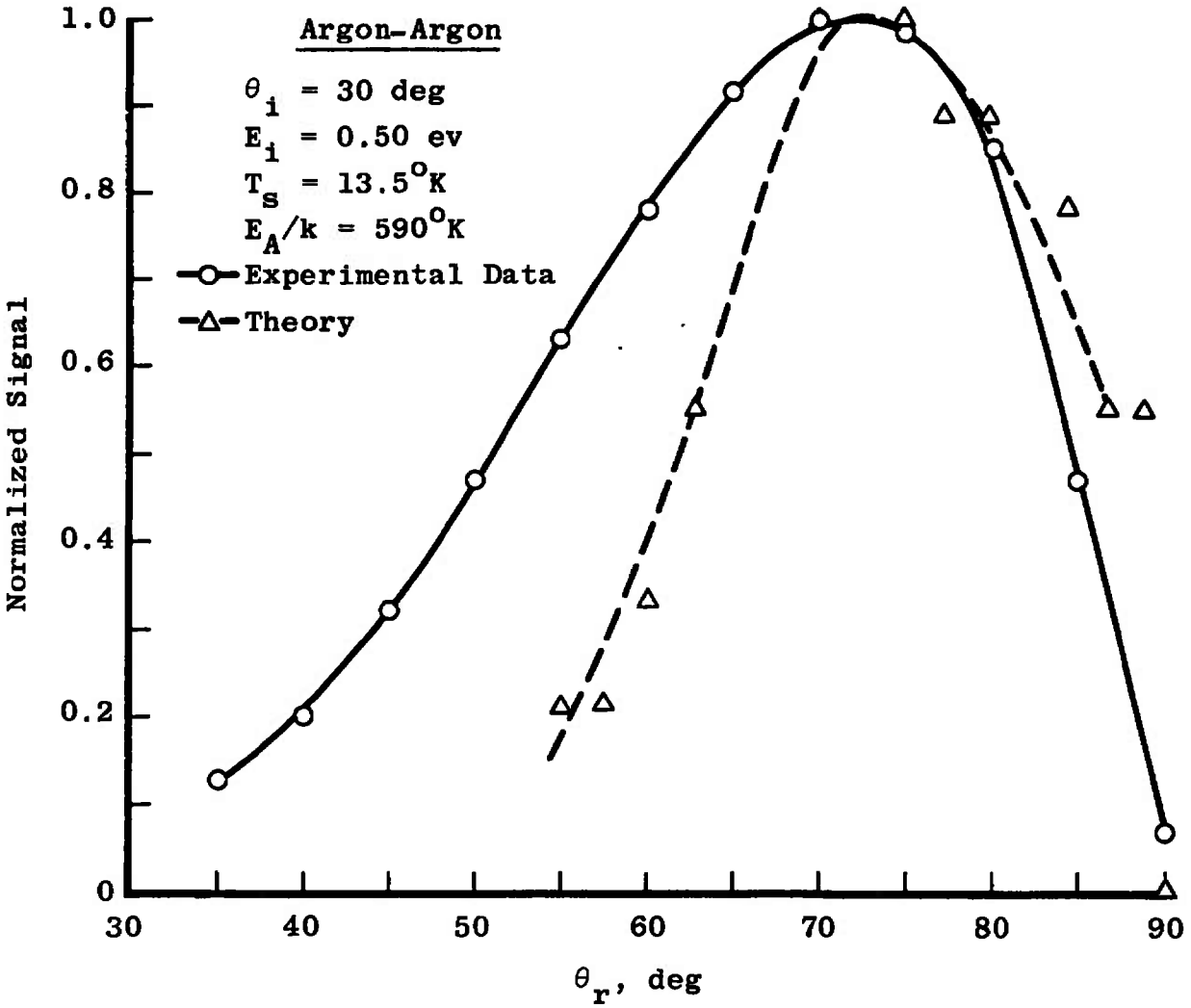

Fig. 25 Normalized In-Plane Spatial Distribution for θ_i = 30 deg and E_i = 0.50 ev

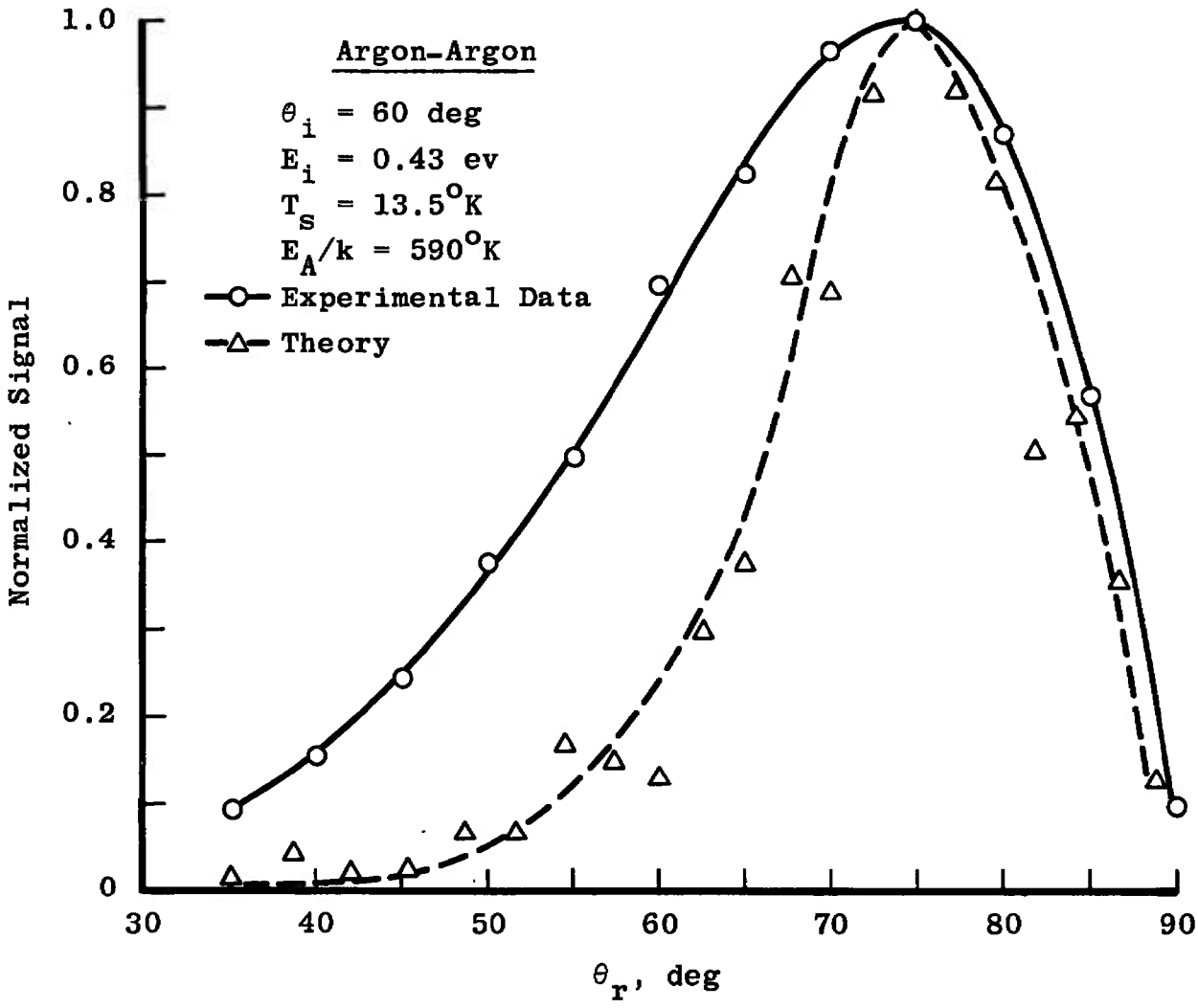

Fig. 26 Normalized In-Plane Spatial Distribution for θ_i = 60 deg and E_i = 0.43 ev

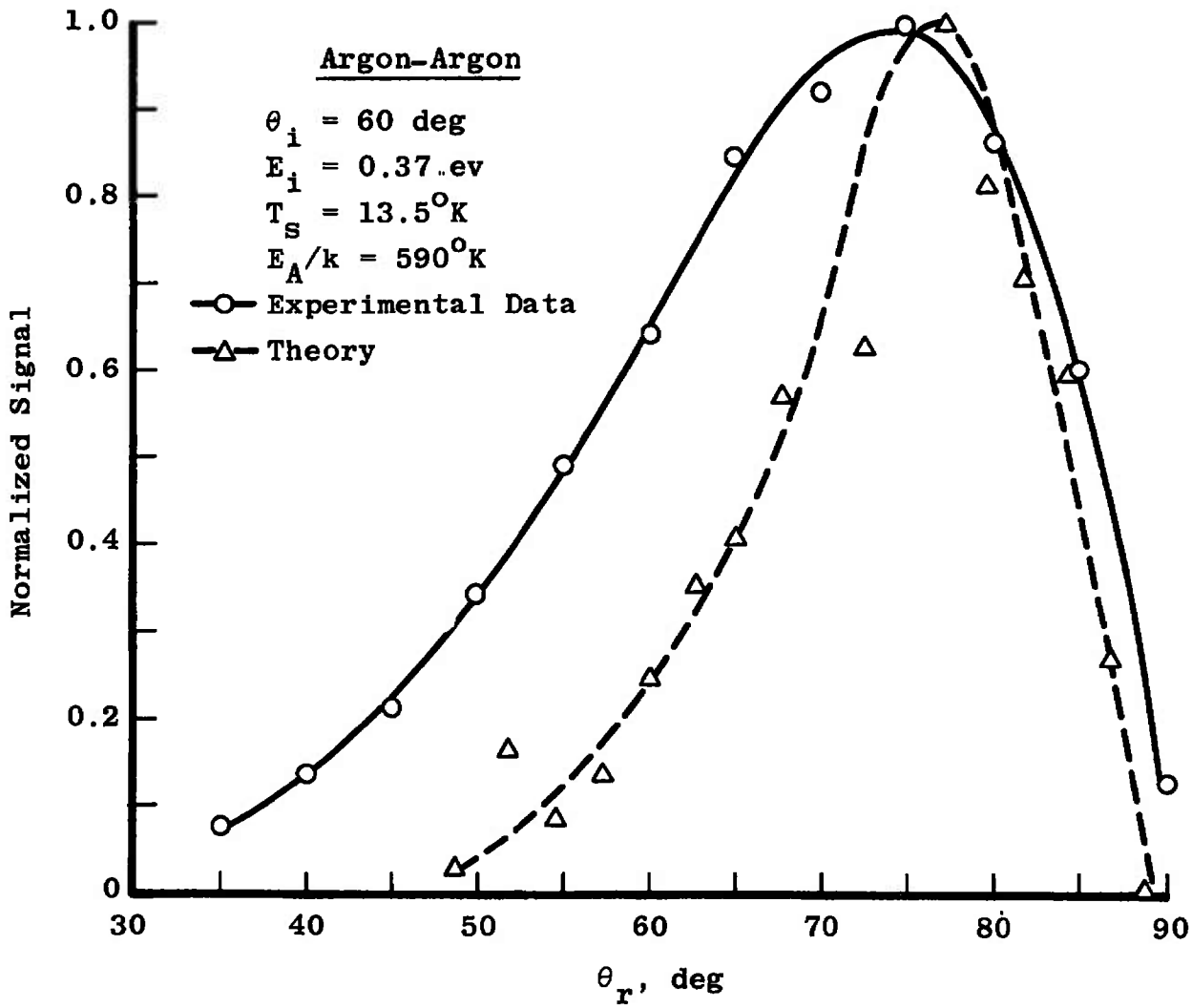

Fig. 27 Normalized In-Plane Spatial Distribution for θ_i = 60 deg and E_i = 0.37 ev

TABLE I
ESTIMATED VALUES OF THE SURFACE FIELD ENERGY BASED ON A LENNARD-JONES POTENTIAL

s, Å	E_A	E_A/k, °K
3.45(σ)	2.14ϵ	257
3.87(r_o)	0.79ϵ	95
3.84(d)	0.81ϵ	97

UNCLASSIFIED

Security Classification

DOCUMENT CONTROL DATA - R & D

(Security classification of title, body of abstract and indexing annotation must be entered when the overall report is classified)

1. ORIGINATING ACTIVITY (Corporate author)	2a. REPORT SECURITY CLASSIFICATION
Arnold Engineering Development Center, ARO, Inc., Operating Contractor, Arnold Air Force Station, Tennessee 37389	UNCLASSIFIED
	2b. GROUP: N/A

3. REPORT TITLE

A CLASSICAL MODEL FOR GAS-SURFACE INTERACTION

4. DESCRIPTIVE NOTES (Type of report and inclusive dates)

July 1969 to March 1970 - Final Report

5. AUTHOR(S) (First name, middle initial, last name)

M. R. Busby, J. D. Haygood, and C. H. Link, Jr., ARO, Inc.

6. REPORT DATE	7a. TOTAL NO. OF PAGES	7b. NO. OF REFS
July 1970	53	15

8a. CONTRACT OR GRANT NO.	9a. ORIGINATOR'S REPORT NUMBER(S)
F40600-69-C-0001	
b. Program Element 64719F	AEDC-TR-70-131
c.	9b. OTHER REPORT NO(S) (Any other numbers that may be assigned this report)
d.	N/A

10. DISTRIBUTION STATEMENT

This document has been approved for public release and sale; its distribution is unlimited.

11. SUPPLEMENTARY NOTES	12. SPONSORING MILITARY ACTIVITY
Available in DDC.	Arnold Engineering Development Center, Air Force Systems Command, Arnold AF Station, Tenn. 37389

13. ABSTRACT

A classical theoretical model for gas-surface interaction has been formulated and tested using the experimental data for the gaseous-argon, solid-argon system. The theoretical interaction is modeled as the collision of hard spheres with the inclusion of surface temperature and an attractive surface field energy which is the only adjustable parameter in the formulation. The theoretical results from this exceedingly simple model exhibit nearly every characteristic of the available experimental data for argon. Several general conclusions about the actual argon-argon interaction were made. First, classical mechanics appeared to provide a useful description for the interaction. Second, a hard sphere model was adequate to predict the gas-solid collision properties over the range of experimental conditions although the theoretical spatial distributions are narrower than those experimentally measured. Third, in order to match the experimental capture coefficient data, the magnitude of the surface field energy was nearer the heat of sublimation rather than the Lennard-Jones or Morse potential well-depth values.

DD FORM 1 NOV 65 1473

UNCLASSIFIED

Security Classification

14. KEY WORDS	LINK A		LINK B		LINK C	
	ROLE	WT	ROLE	WT	ROLE	WT
mathematical model						
gas-molecular flow						
geometric surfaces						
macrostructure						
microstructure						
intermolecular forces						
particle collisions						
Maxwell-Boltzmann distribution						